Published in final edited form as:

Matrix Biol. 2021 May ; 99: 18–42. doi:10.1016/j.matbio.2021.05.005.

Collagen denaturation in the infarcted myocardium involves temporally distinct effects of MT1-MMP-dependent proteolysis and mechanical tension.

Anis Hanna, **Arti V Shinde**, **Ruoshui Li**, **Linda Alex**, **Claudio Humeres**, **Prasanth Balasubramanian**, **Nikolaos G Frangogiannis**

The Wilf Family Cardiovascular Research Institute, Department of Medicine (Cardiology), Albert Einstein College of Medicine, Bronx NY

Abstract

Tissue injury results in profound alterations in the collagen network, associated with unfolding of the collagen triple helix, proteolytic degradation and generation of fragments. In the infarcted myocardium, changes in the collagen network are critically involved in the pathogenesis of left ventricular rupture, adverse remodeling and chronic dysfunction. We hypothesized that myocardial infarction is associated with temporally and spatially restricted patterns of collagen denaturation that may reflect distinct molecular mechanisms of collagen unfolding. We used a mouse model of non-reperfused myocardial infarction, and in vitro assays in fibroblast-populated collagen lattices. In healing infarcts, labeling with collagen hybridizing peptide (CHP) revealed two distinct patterns of collagen denaturation. During the inflammatory and proliferative phases of infarct healing, collagen denaturation was pericellular, localized in close proximity to macrophages and myofibroblasts. qPCR array analysis of genes associated with matrix remodeling showed that Membrane Type 1-Matrix Metalloproteinase (MT1-MMP) is markedly upregulated in infarct macrophages and fibroblasts, suggesting its involvement in pericellular collagen denaturation. In vitro, MT1-MMP-mediated pericellular collagen denaturation is involved in cardiac fibroblast migration. The effects of MT1-MMP on collagen denaturation and fibroblast migration involve the catalytic site, and require hemopexin domain-mediated actions. In contrast, during the maturation phase of infarct healing, extensive collagen denaturation was noted in the hypocellular infarct, in the infarct border zone and in the mitral valve annulus, in the absence of MT1-MMP. In vitro, mechanical tension in attached collagen lattices was sufficient to induce peripheral collagen denaturation. Our study suggests that in healing infarcts, early pericellular collagen denaturation may be important for migration of macrophages and reparative myofibroblasts in the infarct. Extensive denaturation of collagen fibers is noted in mature scars, likely reflecting mechanical tension. Chronic collagen denaturation may increase susceptibility of the matrix to proteolysis, thus contributing to progressive cardiac dilation and post-infarction heart failure.

*Corresponding author: Nikolaos G Frangogiannis, MD, Albert Einstein College of Medicine, 1300 Morris Park Avenue Forchheimer G46B Bronx NY 10461, Tel: 718-430-3546, Fax: 718-430-8989, nikolaos.frangogiannis@einsteinmed.org.

Keywords

myocardial infarction; collagen denaturation; MT1-MMP; fibroblast; macrophage; mechanical tension; collagen hybridizing peptide

INTRODUCTION:

Collagens are the main structural constituents of the extracellular matrix (ECM) in all mammalian tissues. In vertebrates, the collagen superfamily comprises 28 types (type I-XXVIII), that form fibrillar and microfibrillar networks in the parenchymal interstitial matrix and in basement membranes. Collagens not only serve as the main structural components to the fibrillar backbone of the ECM, but can also transduce regulatory signals that modulate cellular behavior[1]. The structural hallmark common to all collagens is the triple helix, an elegant structural motif in which three parallel left-handed polypeptide strands are supercoiled around a central axis in a right-handed manner. This supramolecular structure is stabilized by interstrand hydrogen bonds [2],[3].

The collagen network undergoes dramatic changes in injured and remodeling tissues. Following tissue injury, rapid activation of proteases, including matrix metalloproteinases (MMPs) and cysteine proteinases, degrades collagens, generating fragmented collagen triple helices that spontaneously unfold. Chronic mechanical damage can also trigger collagen unfolding that may be independent of protease-mediated actions. Recently, development of collagen hybridizing peptide (CHP) has contributed a new tool for detection of collagen unfolding in vitro and in vivo. CHP is a small synthetic peptide that mimics the triple-helical structure of native collagens, and hybridizes with denatured unfolded collagen strands, reforming a triple helical structure. Fluorescent and biotin-labeled CHP has been used to report the levels of denatured collagen generated by heat or protease activity [4]. In addition to protease-mediated collagen denaturation, CHP can also detect chronic mechanical damage of collagen. In stretched tendons, mechanical injury generates shear-dominant stress transfer, which pulls one strand out of the collagen triple helix, resulting in unfolding, that is detected through CHP labeling [5].

The adult mammalian heart contains an intricate network of collagenous ECM that provides structural support to the myocardium, while transducing homeostatic signals to myocardial cells. Following myocardial injury, fibroblast-driven expansion of the collagen network plays an important role in cardiac repair, but also contributes to adverse remodeling and fibrosis [6],[7]. Myocardial infarction, the most dramatic and common form of myocardial injury is associated with massive necrosis of cardiomyocytes, and release of damage-associated molecular patterns (DAMPs) that trigger an intense local and systemic inflammatory reaction. Rapid activation of proteases generates matrix fragments with diverse roles in regulation of the inflammatory and fibrogenic response [8],[9]. Some of these matrix fragments have been implicated in recruitment and activation of leukocytes that clear the infarct from dead cells and matrix debris. Phagocytic clearance of apoptotic cells suppresses inflammation and sets the stage for the proliferative phase of infarct healing, associated with myofibroblast activation [10],[11],[12],[13]. Activated

myofibroblasts deposit large amounts of collagens that preserve the structural integrity of the ventricle, preventing catastrophic rupture [14] and secrete matricellular proteins that regulate organization of the structural matrix network [15], and locally modulate growth factor and cytokine signaling and protease activity [16],[17] . Scar maturation follows and is associated with quiescence and deactivation of fibroblasts [18],[19], and with ECM crosslinking [20]. Prevailing concepts suggest that in the infarcted heart, early degradation of collagens is followed by an active collagen-synthetic phase, ultimately leading to formation of a stable mature scar containing large amounts of cross-linked collagen. However, the biochemical changes of the collagen network in infarcted hearts have not been systematically investigated.

We hypothesized that myocardial infarction is associated with temporally and spatially restricted patterns of collagen denaturation that may reflect distinct molecular mechanisms of collagen unfolding. We used CHP labeling to explore the time course, spatial localization and molecular mechanisms of collagen denaturation in infarcted hearts. Using in vitro studies in fibroblasts populating collagen pads and in vivo experiments in a mouse model of myocardial infarction, we found that during the inflammatory and proliferative phase, collagen denaturation is predominantly pericellular, is localized around macrophages and myofibroblasts, and reflects membrane type 1- matrix metalloproteinase (MT1-MMP)-mediated proteolysis by migrating cells. Surprisingly, high levels of denatured collagen were noted in mature scars, reflecting MT1-MMP-independent mechanical stretch. We propose that in infarcted heart, chronic tensile overload of collagen fibers due to elevated intraventricular pressures may increase susceptibility of the matrix to protease-induced degradation causing progressive adverse remodeling.

RESULTS:

1. Use of labeled CHP to identify denatured collagen fibers in the myocardium.

CHP specifically hybridizes with denatured unfolded collagen strands in vitro and in vivo [5],[4]. First, we validated the use of CHP labeling for detection of denatured collagen in the heart. Control hearts exhibited negligible CHP labeling (Supplemental Figure I A–C), reflecting the absence of denatured collagen in the uninjured myocardium. Heat-denatured and proteinase K-treated myocardial sections were used as positive controls and showed CHP staining of the endomysial and perimysial collagenous network, without labeling myocardial cells (Supplemental Figure I D–I). CHP does not bind to newly-synthesized collagen, but hybridizes to globally unfolded strands of collagen I, III and IV [21],[5],[4]. In order to confirm that CHP does not label newly-synthesized collagen, we cultured mouse cardiac fibroblasts in type I collagen lattices and performed dual immunofluorescence for CHP and an anti-collagen type III antibody after 2–6 h of stimulation. After 2 h of stimulation, cardiac fibroblasts exhibited intense synthesis of type III collagen (newly-synthesized) that was not labeled with CHP (Supplemental Figure II).

2. The time course of collagen denaturation following myocardial infarction.

The cardiac reparative response following infarction can be divided into 3 distinct, but overlapping phases: the inflammatory phase, the proliferative phase and the maturation

phase [22]. The inflammatory phase is characterized by infiltration of the infarct zone with leukocytes. During the proliferative phase, activated myofibroblasts become the dominant cell type in the scar and secrete large amounts of ECM proteins. Finally, during the maturation phase, the cellular content of the infarct is reduced and the scar is predominantly comprised of collagenous ECM. Supplemental Figure III shows the time course of changes in the collagen network in non-reperfused mouse myocardial infarcts using picrosirius red staining (Supplemental figure III). During the inflammatory phase of infarct healing (24–72h after infarction), cardiomyocyte death and degradation of the native matrix network triggers recruitment of leukocytes into the infarct zone. During the proliferative phase, suppression of inflammation is accompanied by accumulation of myofibroblasts that secrete extracellular matrix proteins in the infarct and in the border zone (Supplemental Figure III G, H). As the scar matures, the matrix is cross-linked leading to formation of a scar comprised of thick collagen fibers (Supplemental Figure III J). As the infarct heals, the remote non-infarcted myocardium remodels, exhibiting interstitial fibrosis (Supplemental figure III I, L).

In order to study the time course of collagen denaturation in the infarcted mouse heart, we used CHP labeling. During the inflammatory phase (24–72h after coronary occlusion), focal areas of collagen denaturation were found around cells infiltrating the infarct (Figure 1A–L). Quantitative analysis showed that after 24h of coronary occlusion, there was a modest non-significant increase in the levels of denatured collagen, followed by a marked significant increase at the 72h timepoint (****$p<0.0001$, Figure 1M). No significant collagen denaturation was noted in remote remodeling myocardial segments after 24–72h of coronary occlusion (Figure 1A–C, G–I).

During the proliferative phase of cardiac repair (7 days after coronary occlusion), denatured collagen remained predominantly pericellular, and was localized in the subepicardial and subendocardial areas of the infarct and in the infarct border zone (Figure 2A–I).

The pattern of localization of denatured collagen changed during the maturation phase of infarct healing (28 days after coronary occlusion). In mature myocardial scars, a relatively low cellular content is associated with extensive areas of denatured collagen, covering large parts of the ECM in the subepicardial region of the infarct and in the infarct border zone (Figure 2J–R).

Quantitative analysis showed a progressive increase in the levels of denatured collagen during transition from the inflammatory to the proliferative to the maturation phase (Figure 2S). In the mature scar, CHP binding labeled almost 30% of the scar ECM (Figure 2P–R, S) and ~10% of the border zone ECM (Figure 2M–O, S). In contrast, no significant collagen denaturation was noted in the remote remodeling non-infarcted myocardium (Figure 2A–C, J–L, S).

3. During the inflammatory and proliferative phase of cardiac repair, denatured collagen is localized around infiltrating macrophages and myofibroblasts.

Next, we identified the cell types associated with collagen denaturation during the inflammatory and proliferative phases of cardiac repair. Dual staining for the macrophage marker Mac2 and CHP showed that 3 days after coronary occlusion (at the peak of the

inflammatory phase), denatured collagen was predominantly localized in close proximity to macrophages (Figure 3A–F). In contrast, after 7 days of coronary occlusion (during the proliferative phase), infiltrating macrophages were predominantly localized in the center of the infarct and exhibited relatively low levels of pericellular CHP (Figure 3G–L). Quantitative analysis performed using an artificial intelligence-guided model (Supplemental figure IV A–D) showed that the denatured collagen levels around infiltrating macrophages peaked after 3 days of coronary occlusion (Figure 3M–N).

Dual staining for the myofibroblast marker α-SMA and CHP, showed pericellular collagen denaturation around infiltrating myofibroblasts after 72h of coronary occlusion (Figure 4A–F), that increased further after 7 days of coronary occlusion (at the peak of the proliferative phase), as the myofibroblasts localized predominantly in the infarct border zone (Figure 4G–L). Quantitative analysis using an artificial intelligence-guided model (Supplemental figure IV E–H) showed that myofibroblast-associated denatured collagen peaked after 7 days of coronary occlusion (Figure 4M–N).

4. In mature scars, denatured collagen does not exhibit a pericellular localization, but is found in subepicardial collagenous regions of the infarct with low cellular content.

Serial section staining for PicroSirius red and CHP was used to localize denatured collagen in mature myocardial scars after 28 days of coronary occlusion. Moreover, dual fluorescence for Mac2/CHP and for α-SMA/CHP was used to examine potential associations between denatured collagens and macrophages or myofibroblasts. After 28 days of coronary occlusion, a large part of the subepicardial ECM and the infarct border zone was comprised of denatured collagen (Supplemental figure V A–L). In contrast, no significant collagen denaturation was noted in association with myofibroblasts (Supplemental figure V M–O) and macrophages (Supplemental figure V P–R). The extensive collagen denaturation in areas subjected to high mechanical stress, may reflect stretch-induced collagen unfolding.

5. Post-infarction remodeling is associated with extensive collagen denaturation in the remodeling mitral valve.

Although levels of collagen denaturation were very low in the remote remodeling myocardium (Figures 1–2), the mitral valve annulus and leaflets exhibited intense CHP labeling after 7 days of coronary occlusion (Figure 5A–F) that markedly increased after 28 days of coronary occlusion (Figure 5G–J). Post-infarction remodeling is associated with progressive dilation of the left ventricle and mitral valve annular dilation [23], inducing mechanical stress on the valve apparatus. Collagen denaturation in the mitral valve apparatus may reflect mechanical damage of the valvular ECM in the dilated infarcted ventricle.

7. Fibroblasts populating collagen pads induce collagen denaturation that is accentuated following growth factor stimulation.

In order to understand the mechanisms of cell-associated collagen denaturation in healing infarcts, we used an in vitro model of fibroblast-populated collagen pads. First, we examined the time course of changes in cardiac fibroblast morphology and collagen denaturation. Cardiac fibroblasts cultured in pads for 15’−60’ exhibited a round morphology (Figure 6A–D), followed by the development of projections after 2h-6h of culture (Figure 6E–F) and

acquisition of a dendritic morphology after 24h of culture (Figure 6G–H). There was no significant collagen denaturation after 15'−60' of culture. After 2h there was a modest, but significant increase in the levels of denatured collagen. Significant collagen denaturation was noted in peri-fibroblast areas after 6h of culture, and increased dramatically after 24h (Figure 6F–I). At the 24h timepoint, fibroblasts increased in size, became polarized, formed projections and were enmeshed within areas of denatured collagen (Figure 6G–H).

Next, we examined whether stimulation with growth factors, known to be induced and activated in healing infarcts alters the levels of pericellular denatured collagen in fibroblast-populated collagen pads. Stimulation with serum markedly increased the levels of pericellular denatured collagen in fibroblast-populated collagen pads (Figure 7A–F, M). bFGF modestly, but significantly increased collagen denaturation (Figure 7G–I, M). TGF-β1 stimulation also significantly increased the levels of collagen denaturation (Figure 7J–M). Formation of tracks of denatured collagen along the major axis of polarized fibroblasts may reflect collagen processing by cells migrating in the pad.

6. During the inflammatory and proliferative phase of infarct healing, pericellular denatured collagen is associated with MT1-MMP expression by infiltrating cells.

The pericellular localization of CHP during the inflammatory and proliferative phase of infarct healing led us to hypothesize that denatured collagen may reflect protease-mediated processing of the cardiac ECM by migrating macrophages and fibroblasts. In order to identify proteases that may be involved in collagen denaturation, we systematically assessed the expression profile of matrix remodeling genes in infarct macrophages and fibroblasts using a PCR array (Figure 8, Supplemental Figures VI–VII). Control and infarct macrophages harvested at 3 different timepoints (3d, 7d, 28d) had no statistically significant differences in expression levels of *MMP10, MMP2, MMP3, MMP7, MMP8,* and *TIMP1*, but exhibited induction of *MMP12* and *MMP14,* and marked downregulation of *TIMP3* (Figure 8). Fibroblasts harvested from 7-day infarcts also exhibited marked induction of *MMP14* mRNA expression (Figure 8K). MMP14 (MT1-MMP) is the predominant membrane-bound protease involved in matrix breakdown in migrating cells. Considering the marked and consistent upregulation of *MMP14* in infarct macrophages and fibroblasts and the pericellular localization of denatured collagen in the infarct (consistent with degradation in response to a cell-associated protease), we examined whether CHP labeling is associated with MT1-MMP expression. Using dual fluorescent staining for MT1-MMP and CHP, we found that MMP14 expression was associated with pericellular CHP localization during the inflammatory (after 72h of coronary occlusion) and proliferative phase (after 7 days of coronary occlusion) of infarct healing (Supplemental figure VIII A–I). In contrast, in mature scars (after 28 days of coronary occlusion), very high levels of denatured collagen were noted in the absence of MT1-MMP expression (Supplemental figure VIII J–L).

8. Pericellular collagen denaturation in fibroblast-populated pads is dependent on MT1-MMP and is associated with cell migration.

Next, we tested the hypothesis that collagen denaturation is mediated through MT1-MMP. MT1-MMP was sufficient to cause direct collagen I cleavage in a cell-free in vitro model (Supplemental Figure IX). In order to test the hypothesis that pericellular collagen

denaturation is dependent on MT1-MMP expression, we performed MT1-MMP siRNA KD experiments in fibroblasts populating collagen pads. MT1-MMP KD markedly reduced pericellular denatured collagen levels in fibroblasts cultured in collagen pads (Figure 9A–G). In order to explore the mechanism responsible for MT1-MMP effects on denaturation of pericellular collagen, we performed experiments investigating the effects of the catalytic MT1-MMP domain using a specific antibody and of the hemopexin domain, using a functional inhibitor. The hemopexin domain mediates MT1-MMP dimerization [24], an important step in proteinase function and in cell migration [25]. Both hemopexin domain inhibition and catalytic site blockade attenuated collagen denaturation (Figure 9H–I, Supplemental Figure X).

To test the hypothesis that MT1-MMP is involved in cell migration, we performed a fibroblast migration assay using nested collagen pads. MT1-MMP knockdown attenuated fibroblast migration in response to the growth factor PDGF-BB. Moreover, MT1-MMP deficient cells had a trend towards reduced migration in response to serum (Figure 10). Growth factor-mediated fibroblast migration was attenuated by hemopexin domain inhibition (Figure 10H, Supplemental figure XI), and by catalytic site blockade (Figure 10I, Supplemental figure XI). Taken together the findings suggest that MT1-MMP-induced cardiac fibroblast migration involves pericellular collagen denaturation, and may require both protease-dependent actions and hemopexin-domain mediated dimerization

9. Mechanical stress in attached pads increases collagen denaturation in the absence of MT1-MMP.

The abundant collagen denaturation observed in hypocellular regions of the mature scar is independent of MT1-MMP expression and may reflect the direct effects of mechanical stress. To test this hypothesis, we compared denatured collagen levels between free floating collagen pads (in the absence of mechanical tension) and attached collagen lattices, in which the fibroblasts are subjected to mechanical tension[26],[27]. When compared with free-floating pads, attached lattices, exhibit marked increases in the levels of denatured collagen in the edge of the lattice (Figure 11). Collagen denaturation in the edge of attached pads occurred in the absence of MT1-MMP expression (Figure 11J–L).

DISCUSSION:

Our study shows for the first time that collagen denaturation in healing myocardial infarcts is prominent, not only during the highly dynamic inflammatory and proliferative phases, but also in mature scars, which are generally viewed as relatively stable structures that exhibit a low level of cellular activity. Early and late generation of denatured collagen have different patterns of localization and are mediated through distinct underlying mechanisms (Figure 12). During the inflammatory and proliferative phase of infarct healing, denatured collagen is predominantly pericellular, likely reflecting MT1-MMP-mediated migration of infiltrating macrophages and myofibroblasts. In contrast, in the mature scar, collagen denaturation may result from chronic mechanical stretch of the collagenous matrix of the mature scar, or of the collagen network of the mitral valve annulus. Chronic and persistent collagen damage after

a large myocardial infarction may contribute to adverse remodeling and may be involved in the pathogenesis of post-infarction heart failure.

Pericellular collagen denaturation forms a migration path for macrophages and fibroblasts.

Because the adult mammalian heart has negligible regenerative capacity, repair following myocardial infarction is dependent on an inflammatory response and on subsequent activation of reparative myofibroblasts that secrete large amounts of ECM proteins, thus preventing catastrophic rupture. Influx of inflammatory cells and fibroblasts into the infarct zone requires expression of proteolytic enzymes that create a “migration path” for the cells through the native collagenous ECM. Migrating cells express metalloproteinases which enzymatically process the collagenous matrix, creating the path for migration[28]. Our findings show that during the inflammatory and proliferative phases of infarct healing, collagen denaturation is predominantly pericellular, and is localized in close proximity to macrophages (Figure 3) and myofibroblasts (Figure 4).

MT1-MMP mediates collagen denaturation and cell migration

Pericellular collagen denaturation associates with expression of the type I transmembrane proteinase MT1-MMP (Figure 9, Supplemental Figure VIII). Moreover, qPCR arrays examining levels of matrix-remodeling genes showed that MT1-MMP was markedly and consistently upregulated in infarct macrophages and fibroblasts (Figure 8). Of the five MMPs with collagenase activity (MMP1, MMP2, MMP8, MMP13 and MT1-MMP), only MT1-MMP can promote cell migration in a collagen-rich environment [29]. Our in vitro experiments using free-floating fibroblast-populated collagen pads show that pericellular collagen denaturation and fibroblast migration are dependent on MT1-MMP (Figures 9–10). The effects of MT1-MMP on collagen denaturation and fibroblast migration involve both the catalytic site and the hemopexin domain (Figures 9–10). The hemopexin domain mediates homodimerization of MT1-MMP [24], thus mediating cell surface pro-MMP2 activation and promoting cell migration [25]. Cell migration requires processing of the surrounding ECM and involves interactions between the matrix and cell surface integrins [30]. In the healing infarct, MT1-MMP expressed on the migration front of infiltrating cells, may promote cell motility through several distinct mechanisms, including direct denaturation of the collagenous matrix [31],[32],[33], indirect matrix proteolysis through activation of pro-MMP2 and pro-MMP13 [34], or shedding of cell adhesion molecules, such as CD44 [35], and the ectodomain of syndecan-1 [36], or by processing integrins [37]. Non-proteolytic pro-migratory actions of MT1-MMP have also been suggested, involving Hypoxia Inducible Factor (HIF)-1 driven glycolysis necessary for motility-associated metabolic activity [38]. Thus, MT1-MMP may serve as a multifunctional mediator of cell migration [39]. In addition to its role in cell migration and matrix remodeling, MT1-MMP may also activate fibrogenic growth factors through proteolytic processing [40],[41],[42].

The effects of mechanical stress on collagen denaturation

Considering the marked suppression of inflammatory activity noted during the maturation phase of myocardial infarction, accompanied by absence of cell migration, relative quiescence of fibroblasts and matrix cross-linking, we anticipated a reduction in the levels of denatured collagen in mature scars. Surprisingly, despite their relatively low cellular content

in comparison to earlier stages of repair, mature scars had extensive areas of collagen denaturation in the subepicardium and in the infarct border zone (Figure 2, Supplemental figure V), in the absence of MT1-MMP expression. We posited that in the absence of significant cellular migratory or matrix-processing activity, collagen denaturation in mature scars may be related to increased mechanical stress. Experiments using attached fibroblast-populated collagen pads supported this notion. When cultured in attached collagen pads, fibroblasts develop stress fibers and generate mechanical tension[43]. In contrast to the complete absence of denatured collagen in free-floating collagen pads, attached lattices had extensive collagen denaturation in the periphery of the pad (Figure 11), in the absence of MT1-MMP. Much like the ECM in the border zone of a mature infarct, collagen chains located in close proximity to the attachment sites of lattices are subjected to high mechanical tension and exhibit denaturation.

In the infarcted ventricle, mechanical tension of the matrix in the scar is generated in the border zone by contraction of viable cardiomyocytes and is amplified due to the increased intraventricular pressures. Massive loss of contractile myocardium following a large myocardial infarction results in markedly elevated intraventricular pressures, leading to progressive ventricular dilation. As the ventricle remodels, tension in the scar increases. In tendons, sub-rupture tensile overload induced through a protocol of 15 overloading/unloading cycles increased the susceptibility of collagen to trypsin-based collagenolysis. Although the role of overloading vs unloading in collagen denaturation in this model was not systematically investigated, it was suggested that tensile overload may have caused uncoiling of the collagen helix, placing the collagen fibrils in a stable denatured state [44]. The overloading/unloading model of mechanical stress in tendon does not accurately recapitulate the tensile environment in the mature scar, in which the ECM is subjected to contractile forces from viable border zone cardiomyocytes and to perpendicular tension from the increased intraventricular pressure [45],[46]. However, it is tempting to hypothesize that in the mature myocardial scar, mechanical stress may cause denaturation of collagen fibers, increasing their susceptibility to protease-mediated collagenolysis, and contributing to progression of adverse remodeling.

In addition to the infarct zone, we noted extensive collagen denaturation in the mitral valve annulus and leaflets 28 days after coronary occlusion (Figure 5). This finding likely reflects mechanical strain in the annular area, due to marked and progressive dilation of the infarcted ventricle. In animal models of myocardial infarction, dilation of the mitral valve annulus is associated with increased tensile strain[47]. Moreover, development of fibrotic changes in the mitral valve was noted in a sheep model of myocardial infarction, and was accompanied by TGF-β upregulation[48]. These structural changes of the mitral valve may contribute to the pathogenesis of ischemic mitral regurgitation. Moreover, chronic denaturation of collagen fibers in the mitral valve annulus may contribute to the progression of mitral insufficiency following myocardial infarction.

The links between collagen denaturation, ventricular dysfunction and adverse remodeling

What are the functional consequences of collagen denaturation in the infarcted heart? Early denaturation and degradation of collagen during the inflammatory and proliferative

phases of infarct healing may play an important reparative role, facilitating recruitment of macrophages and fibroblasts. Transgenic mice expressing a collagenase-resistant type I collagen exhibited accentuated adverse remodeling, and increased mortality following myocardial infarction, associated with perturbed collagen fibril organization and impaired fibroblast motility [49]. However, excessive or persistent collagen denaturation may have adverse consequences. Extensive experimental evidence suggests that a preserved collagen network protects the heart from early rupture and late dilative remodeling. Mice with a collagen α2(I) mutation that results in complete loss of collagen α2(I) chains, recapitulating human type III osteogenesis imperfecta exhibited an increased incidence of early cardiac rupture [50]. Mice with fibroblast-specific loss of Smad3, a critical TGF-β-induced fibrogenic pathway, had perturbed scar organization and formed a defective matrix network in the infarct zone [14]. On the other hand, direct injection of a collagen implant into the infarct zone thickened the scar and improved systolic function, preventing paradoxical systolic bulging in a rat model of myocardial infarction [51]. Moreover, mice lacking members of the MMP family were protected from cardiac rupture [52],[53] and had attenuated adverse remodeling [54] after myocardial infarction. The protective effects of MMP inhibition may be due, at least in part, to matrix preservation.

Changes in the ECM network may also be involved in the accentuation of adverse post-infarction remodeling associated with aging. Senescent mice had marked reductions in collagen content in the infarct zone [55], that may decrease the tensile strength of the scar, accelerating ventricular dilation and promoting adverse remodeling. The healing defects in senescent hearts were attributed to perturbed growth factor responses [55]. Whether age-related changes in collagen denaturation are implicated in adverse remodeling of infarcted senescent hearts has not been investigated.

Conclusions

Collagen denaturation is prominent in the infarcted heart and can be attributed to two distinct mechanisms. Pericellular collagen denaturation during the inflammatory and proliferative phase of healing is MT1-MMP-dependent, and may be involved in migration of immune cells and reparative fibroblasts into the infarct zone, thus serving a reparative role. In contrast, persistent chronic denaturation of the dense collagen network in the scar, the infarct border zone and the mitral valve apparatus is likely due to mechanical stress, and may promote adverse remodeling and dysfunction, by increasing the susceptibility of the matrix to proteolytic degradation. Approaches aimed at preserving the integrity of the matrix network in remodeling hearts may hold therapeutic promise.

EXPERIMENTAL PROCEDURES:

Experimental model of myocardial infarction.

Animal studies were approved by the Institutional Animal Care and Use Committee at Albert Einstein College of Medicine and conform to the Guide for the Care and Use of Laboratory Animals published by the National Institutes of Health. A model of non-reperfused myocardial infarction induced through coronary ligation was used, as previously described by our group [56]. Female and male C57Bl6J mice, 2–4 months of age, were

anesthetized using inhaled isoflurane (4% for induction, 2% for maintenance). For analgesia, buprenorphine (0.05–0.2 mg/kg s.c) was administered at the time of surgery and q12h thereafter for 2 days. Additional doses of analgesics were given if the animals appeared to be experiencing pain (based on criteria such as immobility and failure to eat). Intraoperatively, heart rate, respiratory rate and electrocardiogram were continuously monitored and the depth of anesthesia was assessed using the toe pinch method. The left anterior descending coronary artery was occluded. Mice were sacrificed after 24h, 72h, 7 days and 28 days of coronary occlusion (n=5/group). Hearts were then harvested for histological analysis, fixed in zinc-formalin (Anatech Ltd., Fisher Scientific) and embedded in paraffin.

Cardiac fibroblast isolation

Mouse hearts were obtained from 12-week-old male and female C57BL/6J mice, were minced, and digested by shaking the tissue fragments in 100 U/ml collagenase CLS 2 (Worthington Biochemical, Lakewood, NJ) for 1 hour at 37°C water bath. Supernatants were filtered multiple times through a 70 μm filter. Cells were passed through the filter were pelleted, washed to remove the collagenase, then resuspended in Dulbecco's modified Eagles medium (DMEM/F12) containing 10% fetal bovine serum (FBS), and antibiotics (PenG 100U/ml, Streptomycin sulfate 100 ug/ml, Amphotericin B 0.25 ug/ml, GIBCO, Grand Island, NY). Cells were then plated on 75-cm^2 flasks, and incubated at 37°C, 5% CO_2. Fibroblasts were used up to passage 2 for stimulation, knockdown and migration experiments.

Fluorescence-activated cell sorting (FACS) of cardiac fibroblasts from control or infarcted hearts

Wild-type C57BL/6J mice underwent 7-day coronary occlusion protocol. Myocardial tissue from control or infarcted hearts of individual mice was then finely minced and suspended in digestion buffer cocktail of collagenase IV (2 mg/mL, Worthington Biochem) and dispase II (1.2U/mL, Stemcell Technologies) in DPBS. Tissue fragments were then incubated at 37°C for 15 minutes with gentle rocking. After incubation, tissue digestion buffer with tissue clusters was triturated by pipetting 10 times using a 10-mL serological pipette. Tissue fragments were again incubated at 37°C and triturated twice more (45 minutes of total digestion time). The final trituration was conducted by pipetting 30× with a p1000 pipette. Cell suspension was filtered through 40 μm cell strainer into 50 mL tubes containing 40 mL DPBS and centrifuged for 20 min at 200g with centrifuge brakes deactivated to remove cell debris. Cells were then resuspended in 5 mL of RBC lysis buffer (eBioscience) and incubate for 5 min at RT. Cell suspension was then centrifuged at 500g for 5 min at RT, and resuspended in Hanks' Balanced Salt Solution (HBSS) containing 2% fetal bovine serum (FBS). Cells in single cell suspensions were blocked with anti-mouse CD16/CD32 (2.5:100, BD Biosciences) for 30 min at 4°C. In order to identify hematopoietic and endothelial cells, the cell suspension was incubated for 1 hour at 4°C with anti-CD45-BV605 (1:100, BioLegend), and anti-CD31-APC-Cy7 (2.5:100, BioLegend). Cell suspension was washed, and labelled with 7-aminoactinomycin D (1:500, Invitrogen) to identify cells with compromised cell membranes. Non-hematopoietic/non-endothelial cells (CD45−/CD31−), which are predominantly fibroblasts [57],[58], were sorted with the

FACSAria (BD Biosciences) and processed for RNA isolation. FlowJo software was used for data analyses.

Isolation of myeloid cells from control or infarcted hearts

Wild-type C57BL/6J mice underwent 3-, 7-, or 28-day coronary occlusion protocols to harvest myeloid cells. Myocardial tissue from control or infarcted hearts of individual mice was finely minced and placed into a digestion buffer cocktail of 0.25 mg/ml Liberase Blendzyme 3 (Roche Applied Science), 20 U/ml DNase I (Sigma-Aldrich), 10 mmol/l HEPES (Invitrogen), and 0.1% sodium azide in HBSS with Ca2+ and Mg2+ (Invitrogen), and shaken at 37°C for 20 minutes. Cells were then passed through a 40-μm nylon mesh. Cell suspension was then centrifuged (10 min, 500 g, 4°C). Up to 108 cells were reconstituted with 200 μL of MACS buffer (Miltenyi Biotec, 130–091-376). Cells in MACS buffer were incubated with 50 μL of Anti-Ly-6G MicroBeads UltraPure (Miltenyi Biotec, Cat. No. 130–092-332) for 10 min at 4°C, and then incubated with 100 μl of anti-biotin microbeads for 15min; washed once and centrifuged. Cells were resuspended in MACS buffer and passed through a MS column (Cat. No. 130–042-201) in a MACS separator (Miltenyi Biotec, 130–090-312). The magnetically labeled Ly6G+ cells were retained on the column. The unlabeled cells (Ly-6G negative flow through) were collected and washed once with MACS buffer (Ly6G- cells) and centrifuged at 500 g for 10 min. Subsequently, the cell pellet (per 10^8 Ly6G– cells) was again resuspended in 90 μL of MACS buffer, incubated with 10 μL of CD11b microBeads (Miltenyi Biotec, Cat. No. 130–049-601) at 4°C for 15 min, and then washed once and centrifuged. Resuspended cells went through a MACS column set in a MACS separator. The magnetically labeled CD11b+ cells were retained on the column. Ly6G-CD11b+ cells (macrophages) were flushed out and harvested for RNA isolation.

Experiments in fibroblast-populated collagen pads

Fibroblasts were cultured in free-floating collagen lattices as previously described by our group [59] Cardiac fibroblasts isolated from adult C57BL/6J mice were cultured to passage 2 and serum-starved overnight (16 h). Collagen matrix was prepared on ice by diluting a stock solution of rat collagen I (3.0 mg/ml) (GIBCO Invitrogen Corporation, Carlsbad, CA) with 2X MEM and distilled water for a final concentration of 1 mg/ml collagen. pH of the solution was then neutralized using 1M NaOH. Cell suspensions in 2X MEM were mixed with collagen solution to achieve the final 3×10^5 cells/ml concentration. Subsequently, 500 μl of this suspension was aliquoted to a 24-well culture plate (BD Falcon, San Jose, CA) and allowed to polymerize at 37°C for 15 min. Following polymerization, pads were released from wells, transferred to 6-well culture plate (BD Falcon, San Jose, CA) and cultured in 10% FCS DMEM/F12 and harvested immediately as control pads or after 15, 30, 60 minutes, 2h, 6h, and 24h. After incubation, the pads were fixed in formalin and processed in paraffin for subsequent histological analysis. For growth factor stimulation experiments, collagen pads were cultured in serum free DMEM/F12 or stimulated with 10% fetal bovine serum, or mouse recombinant TGF-β1 carrier free (10 ng/ml, R&D systems Minneapolis, MN), or basic Fibroblast Growth Factor (50 ng/ml) for 24 h.

Experiments investigating the effects of high tension by comparing attached and free-floating collagen lattices

In order to assess the effects of mechanical tension on collagen denaturation, we used a model of attached fibroblast-populated collagen pads. As described above, cultured cardiac fibroblasts were mixed with neutralized solution of 1 mg/ml collagen I in 2X MEM to achieve the final 3×10^5 cells/ml concentration. Subsequently, 500 μl of this suspension was aliquoted to a 24-well culture plate and allowed to polymerize at 37 °C for 15 min. Following polymerization, collagen pads were either released, or left attached to the edges of the wells. In either condition, pads were incubated with serum free media for 24 hours. After incubation, the attached pads were released, and both free floating and attached pads were fixed in formalin and processed in paraffin for subsequent histological analysis.

siRNA knockdown of MT1-MMP

Small interfering RNA (siRNA) knock down of MT1-MMP was performed as previously described [60]. Briefly, mouse cardiac fibroblasts at passage 2 were seeded at 70% confluence on 6-well plates in DMEM/F12 with 2% FBS. Cells were then transfected with 60 nM of either SMART-pool siRNA to MT1-MMP or a non-silencing control siRNA (Dharmacon) using Lipofectamine® 3000 Reagent (ThermoFisher Scientific) for 48 hours at 37°C, 5% CO_2. Cells were harvested using TrypLE™ Express reagent, counted and populated in collagen pads. Knockdown of MT1-MMP was confirmed by qPCR.

Inhibition of hemopexin and catalytic domains of MT1-MMP

In order to explore the mechanism of MT1-MMP- mediated collagen denaturation and fibroblast migration, we studied the effects of inhibition of hemopexin (HPX) and catalytic domains of MT1-MMP. Mouse cardiac fibroblasts at passage 2 were seeded at 70% confluence on 6-well plates in DMEM/F12 media containing 2% FBS. For inhibition of MT1-MMP HPX domain, cells were treated with the HPX domain inhibitor NSC405020 [61] (100 μM, Millipore-Sigma) or vehicle control (0.1% DMSO) for 24 hours at 37°C, 5% CO_2. For antibody-mediate blockage of MT1-MMP catalytic domain, cells were incubated with the anti-MT1-MMP catalytic domain antibody [62] (20 μg/mL, Millipore-Sigma) or the isotype control for 24 hours at 37°C, 5% CO_2.

Fibroblast migration assay using nested pads

In order to study the role of MT1-MMP in fibroblast migration, a system of fibroblasts migrating through nested collagen lattices was used, based on previously described models [63, 64] . Nested collagen pads consist of two layers of collagen matrices, an inner smaller layer covered by an outer layer. By seeding cells in the inner pad, one can observe cell migration from the inner cellular pad to the outer acellular pad in response to a stimulus in the media surrounding the nested pad (Supplemental figure XII). Fibroblasts were harvested using TrypLE™ Express reagent following siRNA knockdown, Incubation with MT1-MMP HP inhibitor, or blocking of its catalytic domain. Fibroblasts were then counted and mixed with the before-mentioned collagen solution (3×10^5 cells/ml concentration). The mixture was then poured in 24-well plates used as molds to form the inner collagen pad and incubated at 37°C for 15 minutes to induce polymerization of the collagen matrix. 400 μL

of collagen solution was poured in 12-well plates and the polymerized inner pads were placed on top. An additional 600 μL of collagen solution was poured to cover the inner pads. Nested pads were then allowed to polymerize at 37°C for 30 minutes. Nested pads were then detached and were either suspended in serum free DMEM/F12 or stimulated with media containing 10% FBS or 50 ng/ml PDGF-BB for 24h in 6-well plates. Nested pads were used for RNA isolation, or fixed in zinc-formalin (Anatech Ltd., Fisher Scientific) and vertically embedded in paraffin along the thin side of the pad. Pads were then sectioned (5μm thick), stained with Picrosirius red and cells in 10 random fields were quantified to assess migration from the inner to the outer pads.

Assessment of MT1-MMP-mediated collagen denaturation.

In order to study the direct effect of MT1-MMP on collagen denaturation, we studied the cleavage of DQ-Collagen (DQ-Col) by recombinant MT1-MMP. DQ-Col is a fluorescently labelled collagen I that is quenched and only emits fluorescence signal when cleaved [65, 66]. Recombinant MT1-MMP (80 μg/mL, R&D Systems) was activated by recombinant Furin (1.72 μg/mL, R&D Systems) at 37°C for 1.5 h in the activation buffer (50 mM Tris, 1 mM CaCl2, 0.5% (w/v) Brij-35, pH 9.0).

Activated MT1-MMP was diluted to 5 ng/μL in the assay buffer (50 mM Tris, 3 mM CaCl2, 1 μM ZnCl2, pH 8.5), and mixed with DQ-Col (50 μg/mL, ThermoFisher). Activation buffer containing Furin only was used instead of the activated MT1-MMP as a control. 50 μL of the assay mix was loaded to a 96-well plate, and incubated for 1 hour at 37°C. Fluorescence intensity was then recorded using Bio-Tek Synergy microplate reader.

RNA isolation and qPCR

Total RNA was isolated from the nested pads and was reverse transcribed to cDNA using the iScript™ cDNA synthesis kit (Bio-Rad) following the manufacturer's guidelines. Quantitative PCR was performed using SsoFast™ EvaGreen® Supermix (Bio-Rad) on the CFX384™ Real-Time PCR Detection System (Bio-Rad). Primers to detect MT1-MMP were designed using primer BLAST online tool (NIH) and were synthesized by Integrated DNA Technologies (Coralville, IA). The following primer pairs were used: MT1-MMP forward 5'-GGGTTCCTGGCTCATGCCTA -3', reverse 5'-GTGACCCTGACTTGCTTCCATAA-3'.

PCR arrays.

In order to study gene expression in macrophages and fibroblasts harvested from control of infarcted hearts, total RNA was extracted using the TRIzol reagent (Qiagen, 79306). A total of 400 ng of RNA was transcribed into cDNA using the RT^2 first-strand kit (Qiagen, 330404). Quantitative PCR was then performed using the RT^2 Profiler Mouse PCR Array Extracellular Matrix & Adhesion Molecules (PAMM-013ZA-4) from Qiagen according to the manufacturer's protocol. The same thermal profile conditions were used for all primer sets: 95°C for 10 min, 40 cycles at 95°C for 15 s, followed at 60°C for 1 min. The data obtained were analyzed using the ΔCq method. Gene expression levels were normalized to the levels of GAPDH.

Collagen histochemistry:

For histopathological analysis, murine hearts were fixed in zinc-formalin (Z-fix; Anatech, Battle Creek, MI), and embedded in paraffin. Infarcted hearts were sectioned from base to apex at 250 μm intervals, thus reconstructing the whole heart, as previously described [56, 67, 68]. 10 sections (5μm thick) were cut at each level. Picrosirius red staining was used to label the collagen fibers as previously described [67]. Sections were deparaffinized, and stained in picrosirius red solution for 1 hour then dehydrated and mounted. Bright field images and circularly polarized images of picrosirius red-stained sections were obtained using an Axio Imager M2 microscope (Carl Zeiss Microscopy, White Plains NY) as previously described [69].

Assessment of collagen denaturation using collagen hybridizing peptide:

In order to assess denaturation of the collagen network, we used labeling with a peptide that specifically binds to unfolded collagen [4, 70]. A Collagen Hybridizing Peptide 5-FAM conjugate (F-CHP, 3Helix, Inc., Salt Lake City, UT) was used to detect denatured collagen in infarcted heart sections using fluorescent labeling. To validate the use of CHP for labeling of denatured collagen, we used heat-denatured sections by steaming the sections for 25 minutes, and enzymatically-denatured sections by incubating the sections with proteinase-K (10 μg/mL, ThermoFisher) at 37°C for 20 minutes. To assess collagen denaturation in infarcted hearts, sections from infarcted and control hearts were deparaffinized and heat-mediated antigen retrieval was avoided to avoid denaturation of the native collagen in the tissue. Sections were then blocked with 5% BSA for 1 hour. 20 μM dilution of F-CHP was heated for 5 minutes at 80°C, then quenched on ice for 1 minute. Sections were incubated with F-CHP at 4°C overnight. Sections were then washed. Autofluorescence quenching was performed using TrueBlack Lipofuscin Autofluorescence Quencher (23007, Biotium, Fremont, CA). Slides were mounted using Fluoro-Gel II with DAPI (17985, EMS, Hatfield, PA).

In order to examine the spatial relation between denatured collagen and the matrix network we combined CHP staining with wheat germ agglutinin (WGA) lectin histochemistry, using WGA Alexa Fluor 594 conjugate at 1:200 dilution (W11262 Life Technologies Corporation, Eugene OR). WGA labels N-acetylglucosamine (GlcNac) and sialic acid in cell membranes, and secreted proteoglycans in the ECM [71].

Immunohistochemistry:

In order to identify myofibroblasts in the infarct, sections were stained with a mouse anti-α-SMA antibody (1:100 dilution, Sigma, F3777), as previously described [72]. Myofibroblasts were identified as spindle-shaped α-SMA-positive cells located outside the vascular media. Macrophages were stained using rat anti-Mac2 antibody (CL8942AP Cedarlane, Burlington, Canada) in 1:200 dilution, as previously described [56, 73]. The rabbit monoclonal anti mouse MMP14 antibody (ab51074, Abcam, Cambridge, UK) was used to immunolocalize MT1-MMP, and the rabbit anti-Collagen III antibody (ab7778, Abcam, Cambridge, UK) was used to label collagen III. Briefly, sections were deparaffinized and heat-mediated antigen retrieval was performed for 25 minutes while incubating the slides in citrate buffer, pH 6.0 (Sigma, C9999).

This step was avoided when dual CHP labeling and immunohistochemistry was performed to avoid denaturation of the native collagens. Sections were then blocked with 10% serum of the species in which the secondary antibody was raised for 1 hour, and then incubated overnight at 4°C with the primary antibody/CHP solution. Sections were then washed and incubated with a fluorescently labeled secondary antibody for 1 hour at room temperature. Autofluorescence quenching was performed using TrueBlack Lipofuscin Autofluorescence Quencher (23007, Biotium, Fremont, CA). Slides were mounted using Fluoro-Gel II with DAPI (17985, EMS, Hatfield, PA). Slides were then scanned using Zen 2.6 Pro software and the Zeiss Imager M2 microscope (Carl Zeiss Microscopy, White Plains NY).

Machine learning-based quantitative analysis of myofibroblast and macrophage density:

Using default algorithms of the Intellesis Trainable Segmentation module of Zen 2.6 Pro software (Carl Zeiss Microscopy, New York NY), an artificial intelligence (AI)-based model was trained on multiple fields of different regions of the myocardium to segment the images and identify myofibroblasts, as previously described [74]. Objects of interest were defined as the DAPI-positive nuclei surrounded by α-SMA profiles, excluding vascular smooth muscle cells (VSMCs). The unstained myocardium (including VSMCs) was considered the background. Using Image Analysis module, specific settings were incorporated in the trained model to count the segmented objects. Similarly, an AI-based model was trained to segment the images and identify macrophages. DAPI/Mac2 double positive objects were identified as the objects of interest while the unstained myocardium was considered the background. Using Image Analysis module, specific settings were incorporated in the trained model to count the segmented objects. Automatic analysis of 30–40 fields from two different levels of the murine heart was performed using the trained models.

Machine learning-based quantitative analysis of collagen denaturation:

AI-based models were trained to segment CHP-stained areas using Intellesis module of Zen Pro software (Carl Zeiss Microscopy, White Plains NY). Specific settings in Image Analysis module of Zen Pro software were then incorporated in the trained models to measure surface areas of the segmented objects. First, a model was trained to segment the colocalization of CHP and WGA in control or infarcted hearts at 24h, 72h, 7 days and 28 days following infarction. Automatic analysis of 15–20 fields from two different levels was performed and surface area of CHP/WGA colocalization was reported as percentage to the tissue surface area. Second, another model was trained to segment CHP-stained areas in mitral valve. Automatic analysis of 5–10 fields containing the mitral valve was then performed using the trained model, and surface area of CHP was reported as percentage of tissue area. Third, another AI-based model was trained to identify peri-myofibroblast and peri-macrophage CHP staining that was defined as CHP labeling in direct contact with cell bodies. The aim was to semi-quantitatively identify which cell type has higher pericellular collagen denaturation at 3, and 7 days following infarction. Automatic analysis of 15–20 fields from two different levels of the murine heart was then performed using the trained model, and CHP areas divided by cell densities were reported. Forth, a similar model was trained to segment pericellular CHP labeling in fibroblast-populated collagen pads. Automatic analysis of 15–20 fields from two levels in the collagen pads was then performed and pericellular CHP-stained area per cell was reported. Fifth, CHP labeling of the free floating or attached

collagen pads was segmented using another AI-based model. Automatic analysis of 15–20 fields from two levels in the collagen pads was then performed and surface area of CHP was reported as percentage to collagen pad surface area per field.

Machine learning-based quantitative analysis of collagen surface area following infarction:

In order to study the time course of collagen deposition following myocardial infarction, an AI-based model was trained to segment Sirius red stained fibers using Intellesis module of Zen Pro software (Carl Zeiss Microscopy, White Plains NY). Specific settings in Image Analysis module of Zen Pro software were then incorporated in the trained models to measure surface areas of the segmented objects, and produce the percentage of Sirius red stained area to the total area of the field in control hearts or at 24h, 72h, 7 days and 28 days following infarction. Automatic analysis of 15–20 fields from two different levels was performed and surface area of Sirius red stained fibers was reported as percentage to the tissue surface area.

Statistical analysis:

For all analyses, normal distribution was tested using the Shapiro-Wilk normality test. For comparisons of two groups unpaired, 2-tailed Student's t-test using (when appropriate) Welch's correction for unequal variances was performed. The Mann-Whitney test was used for comparisons between 2 groups that did not show Gaussian distribution. For comparisons of multiple groups, 1-way ANOVA was performed followed by Tukey's multiple comparison test. The Kruskal-Wallis test, followed by Dunn's multiple comparison post-test was used when one or more groups did not show Gaussian distribution. Data are expressed as means ± SEM. Statistical significance was set at 0.05.

Supplementary Material

Refer to Web version on PubMed Central for supplementary material.

SOURCES OF FUNDING:

Dr Frangogiannis' laboratory is supported by National Institutes of Health grants R01 HL76246, R01 HL85440, and R01 HL149407, and by U.S. Department of Defense grant PR181464. Dr Hanna is supported by AHA post-doctoral award 831084. Dr Humeres was supported by AHA post-doctoral award 19POST34450144. Ruoshui Li is sponsored by the China Scholarship Council.

REFERENCES:

[1]. Gelse K, Poschl E, Aigner T, Collagens--structure, function, and biosynthesis, Adv Drug Deliv Rev, 55 (2003) 1531–1546. [PubMed: 14623400]

[2]. Fidler AL, Boudko SP, Rokas A, Hudson BG, The triple helix of collagens - an ancient protein structure that enabled animal multicellularity and tissue evolution, J Cell Sci, 131 (2018).

[3]. Shoulders MD, Raines RT, Collagen structure and stability, Annu Rev Biochem, 78 (2009) 929–958. [PubMed: 19344236]

[4]. Hwang J, Huang Y, Burwell TJ, Peterson NC, Connor J, Weiss SJ, Yu SM, Li Y, In Situ Imaging of Tissue Remodeling with Collagen Hybridizing Peptides, ACS Nano, 11 (2017) 9825–9835. [PubMed: 28877431]

[5]. Zitnay JL, Li Y, Qin Z, San BH, Depalle B, Reese SP, Buehler MJ, Yu SM, Weiss JA, Molecular level detection and localization of mechanical damage in collagen enabled by collagen hybridizing peptides, Nature communications, 8 (2017) 14913.

[6]. Humeres C, Frangogiannis NG, Fibroblasts in the Infarcted, Remodeling, and Failing Heart, JACC Basic Transl Sci, 4 (2019) 449–467. [PubMed: 31312768]

[7]. French BA, Holmes JW, Implications of scar structure and mechanics for post-infarction cardiac repair and regeneration, Exp Cell Res, 376 (2019) 98–103. [PubMed: 30610848]

[8]. de Castro Bras LE, Frangogiannis NG, Extracellular matrix-derived peptides in tissue remodeling and fibrosis, Matrix Biol, 91–92 (2020) 176–187.

[9]. Lindsey ML, Iyer RP, Zamilpa R, Yabluchanskiy A, DeLeon-Pennell KY, Hall ME, Kaplan A, Zouein FA, Bratton D, Flynn ER, Cannon PL, Tian Y, Jin YF, Lange RA, Tokmina-Roszyk D, Fields GB, de Castro Bras LE, A Novel Collagen Matricryptin Reduces Left Ventricular Dilation Post-Myocardial Infarction by Promoting Scar Formation and Angiogenesis, J Am Coll Cardiol, 66 (2015) 1364–1374. [PubMed: 26383724]

[10]. Daseke MJ 2nd, Tenkorang MAA, Chalise U, Konfrst SR, Lindsey ML, Cardiac fibroblast activation during myocardial infarction wound healing: Fibroblast polarization after MI, Matrix Biol, 91–92 (2020) 109–116.

[11]. Pakshir P, Noskovicova N, Lodyga M, Son DO, Schuster R, Goodwin A, Karvonen H, Hinz B, The myofibroblast at a glance, J Cell Sci, 133 (2020).

[12]. Bretherton R, Bugg D, Olszewski E, Davis J, Regulators of cardiac fibroblast cell state, Matrix Biol, 91–92 (2020) 117–135.

[13]. Stempien-Otero A, Kim DH, Davis J, Molecular networks underlying myofibroblast fate and fibrosis, J Mol Cell Cardiol, 97 (2016) 153–161. [PubMed: 27167848]

[14]. Kong P, Shinde AV, Su Y, Russo I, Chen B, Saxena A, Conway SJ, Graff JM, Frangogiannis NG, Opposing Actions of Fibroblast and Cardiomyocyte Smad3 Signaling in the Infarcted Myocardium, Circulation, 137 (2018) 707–724. [PubMed: 29229611]

[15]. McCurdy S, Baicu CF, Heymans S, Bradshaw AD, Cardiac extracellular matrix remodeling: fibrillar collagens and Secreted Protein Acidic and Rich in Cysteine (SPARC), J Mol Cell Cardiol, 48 (2010) 544–549. [PubMed: 19577572]

[16]. Frangogiannis NG, The extracellular matrix in myocardial injury, repair, and remodeling, J Clin Invest, 127 (2017) 1600–1612. [PubMed: 28459429]

[17]. Murphy-Ullrich JE, Sage EH, Revisiting the matricellular concept, Matrix Biol, 37 (2014) 1–14. [PubMed: 25064829]

[18]. Fu X, Khalil H, Kanisicak O, Boyer JG, Vagnozzi RJ, Maliken BD, Sargent MA, Prasad V, Valiente-Alandi I, Blaxall BC, Molkentin JD, Specialized fibroblast differentiated states underlie scar formation in the infarcted mouse heart, J Clin Invest, 128 (2018) 2127–2143. [PubMed: 29664017]

[19]. Frangogiannis NG, Michael LH, Entman ML, Myofibroblasts in reperfused myocardial infarcts express the embryonic form of smooth muscle myosin heavy chain (SMemb), Cardiovasc Res, 48 (2000) 89–100. [PubMed: 11033111]

[20]. Gonzalez-Santamaria J, Villalba M, Busnadiego O, Lopez-Olaneta MM, Sandoval P, Snabel J, Lopez-Cabrera M, Erler JT, Hanemaaijer R, Lara-Pezzi E, Rodriguez-Pascual F, Matrix cross-linking lysyl oxidases are induced in response to myocardial infarction and promote cardiac dysfunction, Cardiovasc Res, 109 (2016) 67–78. [PubMed: 26260798]

[21]. Li Y, Foss CA, Summerfield DD, Doyle JJ, Torok CM, Dietz HC, Pomper MG, Yu SM, Targeting collagen strands by photo-triggered triple-helix hybridization, Proc Natl Acad Sci U S A, 109 (2012) 14767–14772. [PubMed: 22927373]

[22]. Dewald O, Ren G, Duerr GD, Zoerlein M, Klemm C, Gersch C, Tincey S, Michael LH, Entman ML, Frangogiannis NG, Of mice and dogs: species-specific differences in the inflammatory response following myocardial infarction, Am J Pathol, 164 (2004) 665–677. [PubMed: 14742270]

[23]. Watanabe N, Ogasawara Y, Yamaura Y, Wada N, Kawamoto T, Toyota E, Akasaka T, Yoshida K, Mitral annulus flattens in ischemic mitral regurgitation: geometric differences between

inferior and anterior myocardial infarction: a real-time 3-dimensional echocardiographic study, Circulation, 112 (2005) I458–462. [PubMed: 16159863]

[24]. Itoh Y, Takamura A, Ito N, Maru Y, Sato H, Suenaga N, Aoki T, Seiki M, Homophilic complex formation of MT1-MMP facilitates proMMP-2 activation on the cell surface and promotes tumor cell invasion, EMBO J, 20 (2001) 4782–4793. [PubMed: 11532942]

[25]. Itoh Y, Palmisano R, Anilkumar N, Nagase H, Miyawaki A, Seiki M, Dimerization of MT1-MMP during cellular invasion detected by fluorescence resonance energy transfer, Biochem J, 440 (2011) 319–326. [PubMed: 21846327]

[26]. Tomasek JJ, Gabbiani G, Hinz B, Chaponnier C, Brown RA, Myofibroblasts and mechano-regulation of connective tissue remodelling, Nat Rev Mol Cell Biol, 3 (2002) 349–363. [PubMed: 11988769]

[27]. Kolodney MS, Wysolmerski RB, Isometric contraction by fibroblasts and endothelial cells in tissue culture: a quantitative study, J Cell Biol, 117 (1992) 73–82. [PubMed: 1556157]

[28]. Pilcher BK, Dumin JA, Sudbeck BD, Krane SM, Welgus HG, Parks WC, The activity of collagenase-1 is required for keratinocyte migration on a type I collagen matrix, J Cell Biol, 137 (1997) 1445–1457. [PubMed: 9182674]

[29]. Hotary K, Allen E, Punturieri A, Yana I, Weiss SJ, Regulation of cell invasion and morphogenesis in a three-dimensional type I collagen matrix by membrane-type matrix metalloproteinases 1, 2, and 3, J Cell Biol, 149 (2000) 1309–1323. [PubMed: 10851027]

[30]. Kanda S, Kuzuya M, Ramos MA, Koike T, Yoshino K, Ikeda S, Iguchi A, Matrix metalloproteinase and alphavbeta3 integrin-dependent vascular smooth muscle cell invasion through a type I collagen lattice, Arterioscler Thromb Vasc Biol, 20 (2000) 998–1005. [PubMed: 10764664]

[31]. Favreau AJ, Vary CP, Brooks PC, Sathyanarayana P, Cryptic collagen IV promotes cell migration and adhesion in myeloid leukemia, Cancer Med, 3 (2014) 265–272. [PubMed: 24519883]

[32]. Sato H, Takino T, Coordinate action of membrane-type matrix metalloproteinase-1 (MT1-MMP) and MMP-2 enhances pericellular proteolysis and invasion, Cancer Sci, 101 (2010) 843–847. [PubMed: 20148894]

[33]. Guo C, Piacentini L, Type I collagen-induced MMP-2 activation coincides with up-regulation of membrane type 1-matrix metalloproteinase and TIMP-2 in cardiac fibroblasts, J Biol Chem, 278 (2003) 46699–46708. [PubMed: 12970340]

[34]. Knauper V, Will H, Lopez-Otin C, Smith B, Atkinson SJ, Stanton H, Hembry RM, Murphy G, Cellular mechanisms for human procollagenase-3 (MMP-13) activation. Evidence that MT1-MMP (MMP-14) and gelatinase a (MMP-2) are able to generate active enzyme, J Biol Chem, 271 (1996) 17124–17131. [PubMed: 8663255]

[35]. Kajita M, Itoh Y, Chiba T, Mori H, Okada A, Kinoh H, Seiki M, Membrane-type 1 matrix metalloproteinase cleaves CD44 and promotes cell migration, J Cell Biol, 153 (2001) 893–904. [PubMed: 11381077]

[36]. Endo K, Takino T, Miyamori H, Kinsen H, Yoshizaki T, Furukawa M, Sato H, Cleavage of syndecan-1 by membrane type matrix metalloproteinase-1 stimulates cell migration, J Biol Chem, 278 (2003) 40764–40770. [PubMed: 12904296]

[37]. Baciu PC, Suleiman EA, Deryugina EI, Strongin AY, Membrane type-1 matrix metalloproteinase (MT1-MMP) processing of pro-alphav integrin regulates cross-talk between alphavbeta3 and alpha2beta1 integrins in breast carcinoma cells, Exp Cell Res, 291 (2003) 167–175. [PubMed: 14597417]

[38]. Sakamoto T, Seiki M, A membrane protease regulates energy production in macrophages by activating hypoxia-inducible factor-1 via a non-proteolytic mechanism, J Biol Chem, 285 (2010) 29951–29964. [PubMed: 20663879]

[39]. Gifford V, Itoh Y, MT1-MMP-dependent cell migration: proteolytic and non-proteolytic mechanisms, Biochem Soc Trans, 47 (2019) 811–826. [PubMed: 31064864]

[40]. Zavadzkas JA, Mukherjee R, Rivers WT, Patel RK, Meyer EC, Black LE, McKinney RA, Oelsen JM, Stroud RE, Spinale FG, Direct regulation of membrane type 1 matrix metalloproteinase following myocardial infarction causes changes in survival, cardiac function, and remodeling, Am J Physiol Heart Circ Physiol, 301 (2011) H1656–1666. [PubMed: 21666120]

[41]. Dixon JA, Gaillard WF 2nd, Rivers WT, Koval CN, Stroud RE, Mukherjee R, Spinale FG, Heterogeneity in MT1-MMP activity with ischemia-reperfusion and previous myocardial infarction: relation to regional myocardial function, Am J Physiol Heart Circ Physiol, 299 (2010) H1947–1958. [PubMed: 20935147]

[42]. Spinale FG, Mukherjee R, Zavadzkas JA, Koval CN, Bouges S, Stroud RE, Dobrucki LW, Sinusas AJ, Cardiac restricted overexpression of membrane type-1 matrix metalloproteinase causes adverse myocardial remodeling following myocardial infarction, J Biol Chem, 285 (2010) 30316–30327. [PubMed: 20643648]

[43]. Tomasek JJ, Haaksma CJ, Eddy RJ, Vaughan MB, Fibroblast contraction occurs on release of tension in attached collagen lattices: dependency on an organized actin cytoskeleton and serum, Anat Rec, 232 (1992) 359–368. [PubMed: 1543260]

[44]. Veres SP, Harrison JM, Lee JM, Mechanically overloading collagen fibrils uncoils collagen molecules, placing them in a stable, denatured state, Matrix Biol, 33 (2014) 54–59. [PubMed: 23880369]

[45]. Fomovsky GM, Rouillard AD, Holmes JW, Regional mechanics determine collagen fiber structure in healing myocardial infarcts, J Mol Cell Cardiol, 52 (2012) 1083–1090. [PubMed: 22418281]

[46]. Holmes JW, Borg TK, Covell JW, Structure and mechanics of healing myocardial infarcts, Annu Rev Biomed Eng, 7 (2005) 223–253. [PubMed: 16004571]

[47]. Rausch MK, Tibayan FA, Ingels NB Jr., Miller DC, Kuhl E, Mechanics of the mitral annulus in chronic ischemic cardiomyopathy, Ann Biomed Eng, 41 (2013) 2171–2180. [PubMed: 23636575]

[48]. Beaudoin J, Dal-Bianco JP, Aikawa E, Bischoff J, Guerrero JL, Sullivan S, Bartko PE, Handschumacher MD, Kim DH, Wylie-Sears J, Aaron J, Levine RA, Mitral Leaflet Changes Following Myocardial Infarction: Clinical Evidence for Maladaptive Valvular Remodeling, Circ Cardiovasc Imaging, 10 (2017).

[49]. Nong Z, O'Neil C, Lei M, Gros R, Watson A, Rizkalla A, Mequanint K, Li S, Frontini MJ, Feng Q, Pickering JG, Type I collagen cleavage is essential for effective fibrotic repair after myocardial infarction, Am J Pathol, 179 (2011) 2189–2198. [PubMed: 21907695]

[50]. Hofmann U, Bonz A, Frantz S, Hu K, Waller C, Roemer K, Wolf J, Gattenlohner S, Bauersachs J, Ertl G, A collagen alpha2(I) mutation impairs healing after experimental myocardial infarction, Am J Pathol, 180 (2012) 113–122. [PubMed: 22067913]

[51]. Dai W, Wold LE, Dow JS, Kloner RA, Thickening of the infarcted wall by collagen injection improves left ventricular function in rats: a novel approach to preserve cardiac function after myocardial infarction, J Am Coll Cardiol, 46 (2005) 714–719. [PubMed: 16098441]

[52]. Heymans S, Luttun A, Nuyens D, Theilmeier G, Creemers E, Moons L, Dyspersin GD, Cleutjens JP, Shipley M, Angellilo A, Levi M, Nube O, Baker A, Keshet E, Lupu F, Herbert JM, Smits JF, Shapiro SD, Baes M, Borgers M, Collen D, Daemen MJ, Carmeliet P, Inhibition of plasminogen activators or matrix metalloproteinases prevents cardiac rupture but impairs therapeutic angiogenesis and causes cardiac failure, Nat Med, 5 (1999) 1135–1142. [PubMed: 10502816]

[53]. Matsumura S, Iwanaga S, Mochizuki S, Okamoto H, Ogawa S, Okada Y, Targeted deletion or pharmacological inhibition of MMP-2 prevents cardiac rupture after myocardial infarction in mice, J Clin Invest, 115 (2005) 599–609. [PubMed: 15711638]

[54]. Ducharme A, Frantz S, Aikawa M, Rabkin E, Lindsey M, Rohde LE, Schoen FJ, Kelly RA, Werb Z, Libby P, Lee RT, Targeted deletion of matrix metalloproteinase-9 attenuates left ventricular enlargement and collagen accumulation after experimental myocardial infarction, J Clin Invest, 106 (2000) 55–62. [PubMed: 10880048]

[55]. Bujak M, Kweon HJ, Chatila K, Li N, Taffet G, Frangogiannis NG, Aging-related defects are associated with adverse cardiac remodeling in a mouse model of reperfused myocardial infarction, J Am Coll Cardiol, 51 (2008) 1384–1392. [PubMed: 18387441]

[56]. Chen B, Huang S, Su Y, Wu YJ, Hanna A, Brickshawana A, Graff J, Frangogiannis NG, Macrophage Smad3 Protects the Infarcted Heart, Stimulating Phagocytosis and Regulating Inflammation, Circ Res, 125 (2019) 55–70. [PubMed: 31092129]

[57]. Pinto AR, Ilinykh A, Ivey MJ, Kuwabara JT, D'Antoni ML, Debuque R, Chandran A, Wang L, Arora K, Rosenthal NA, Tallquist MD, Revisiting Cardiac Cellular Composition, Circ Res, 118 (2016) 400–409. [PubMed: 26635390]

[58]. Saxena A, Chen W, Su Y, Rai V, Uche OU, Li N, Frangogiannis NG, IL-1 Induces Proinflammatory Leukocyte Infiltration and Regulates Fibroblast Phenotype in the Infarcted Myocardium, J Immunol, 191 (2013) 4838–4848. [PubMed: 24078695]

[59]. Shinde AV, Humeres C, Frangogiannis NG, The role of alpha-smooth muscle actin in fibroblast-mediated matrix contraction and remodeling, Biochim Biophys Acta, 1863 (2017) 298–309.

[60]. Huang S, Chen B, Humeres C, Alex L, Hanna A, Frangogiannis NG, The role of Smad2 and Smad3 in regulating homeostatic functions of fibroblasts in vitro and in adult mice, Biochim Biophys Acta Mol Cell Res, 1867 (2020) 118703. [PubMed: 32179057]

[61]. Remacle AG, Golubkov VS, Shiryaev SA, Dahl R, Stebbins JL, Chernov AV, Cheltsov AV, Pellecchia M, Strongin AY, Novel MT1-MMP small-molecule inhibitors based on insights into hemopexin domain function in tumor growth, Cancer Res, 72 (2012) 2339–2349. [PubMed: 22406620]

[62]. Sathyamoorthy T, Tezera LB, Walker NF, Brilha S, Saraiva L, Mauri FA, Wilkinson RJ, Friedland JS, Elkington PT, Membrane Type 1 Matrix Metalloproteinase Regulates Monocyte Migration and Collagen Destruction in Tuberculosis, J Immunol, 195 (2015) 882–891. [PubMed: 26091717]

[63]. Grinnell F, Rocha LB, Iucu C, Rhee S, Jiang H, Nested collagen matrices: a new model to study migration of human fibroblast populations in three dimensions, Exp Cell Res, 312 (2006) 86–94. [PubMed: 16256985]

[64]. Jiang H, Rhee S, Ho CH, Grinnell F, Distinguishing fibroblast promigratory and procontractile growth factor environments in 3-D collagen matrices, FASEB J, 22 (2008) 2151–2160. [PubMed: 18272655]

[65]. Sloane BF, Sameni M, Podgorski I, Cavallo-Medved D, Moin K, Functional imaging of tumor proteolysis, Annu Rev Pharmacol Toxicol, 46 (2006) 301–315. [PubMed: 16402907]

[66]. Sameni M, Cavallo-Medved D, Dosescu J, Jedeszko C, Moin K, Mullins SR, Olive MB, Rudy D, Sloane BF, Imaging and quantifying the dynamics of tumor-associated proteolysis, Clin Exp Metastasis, 26 (2009) 299–309. [PubMed: 19082919]

[67]. Russo I, Cavalera M, Huang S, Su Y, Hanna A, Chen B, Shinde AV, Conway SJ, Graff J, Frangogiannis NG, Protective Effects of Activated Myofibroblasts in the Pressure-Overloaded Myocardium Are Mediated Through Smad-Dependent Activation of a Matrix-Preserving Program, Circ Res, 124 (2019) 1214–1227. [PubMed: 30686120]

[68]. Christia P, Bujak M, Gonzalez-Quesada C, Chen W, Dobaczewski M, Reddy A, Frangogiannis NG, Systematic characterization of myocardial inflammation, repair, and remodeling in a mouse model of reperfused myocardial infarction, J Histochem Cytochem, 61 (2013) 555–570. [PubMed: 23714783]

[69]. Shinde AV, Dobaczewski M, de Haan JJ, Saxena A, Lee KK, Xia Y, Chen W, Su Y, Hanif W, Kaur Madahar I, Paulino VM, Melino G, Frangogiannis NG, Tissue transglutaminase induction in the pressure-overloaded myocardium regulates matrix remodelling, Cardiovasc Res, 113 (2017) 892–905. [PubMed: 28371893]

[70]. Li Y, Yu SM, Targeting and mimicking collagens via triple helical peptide assembly, Curr Opin Chem Biol, 17 (2013) 968–975. [PubMed: 24210894]

[71]. Karlsson A, Wheat germ agglutinin induces NADPH-oxidase activity in human neutrophils by interaction with mobilizable receptors, Infect Immun, 67 (1999) 3461–3468. [PubMed: 10377127]

[72]. Shinde AV, Humeres C, Frangogiannis NG, The role of alpha-smooth muscle actin in fibroblast-mediated matrix contraction and remodeling, Biochim Biophys Acta Mol Basis Dis, 1863 (2017) 298–309. [PubMed: 27825850]

[73]. Frunza O, Russo I, Saxena A, Shinde AV, Humeres C, Hanif W, Rai V, Su Y, Frangogiannis NG, Myocardial Galectin-3 Expression Is Associated with Remodeling of the Pressure-Overloaded Heart and May Delay the Hypertrophic Response without Affecting Survival, Dysfunction, and Cardiac Fibrosis, Am J Pathol, 186 (2016) 1114–1127. [PubMed: 26948424]

[74]. Hanna A, Shinde AV, Frangogiannis NG, Validation of diagnostic criteria and histopathological characterization of cardiac rupture in the mouse model of nonreperfused myocardial infarction, Am J Physiol Heart Circ Physiol, 319 (2020) H948–H964. [PubMed: 32886000]

HIGHLIGHTS:

- In healing infarcts, collagen denaturation exhibits two distinct phases.
- During the inflammatory and proliferative phases, collagen denaturation is pericellular, localized in close proximity to macrophages and myofibroblasts.
- Early pericellular collagen denaturation reflects Membrane Type 1- Matrix Metalloproteinase (MT1-MMP)-induced proteolysis and cell migration
- MT1-MMP-mediated effects on collagen denaturation and fibroblast migration involve the catalytic site and the hemopexin domain.
- Mechanical tension may be responsible for MT1-MMP-independent collagen denaturation during the maturation phase of infarct healing.
- Chronic collagen denaturation may increase susceptibility of the matrix to proteolysis, thus contributing to progressive cardiac dilation and post-infarction heart failure.

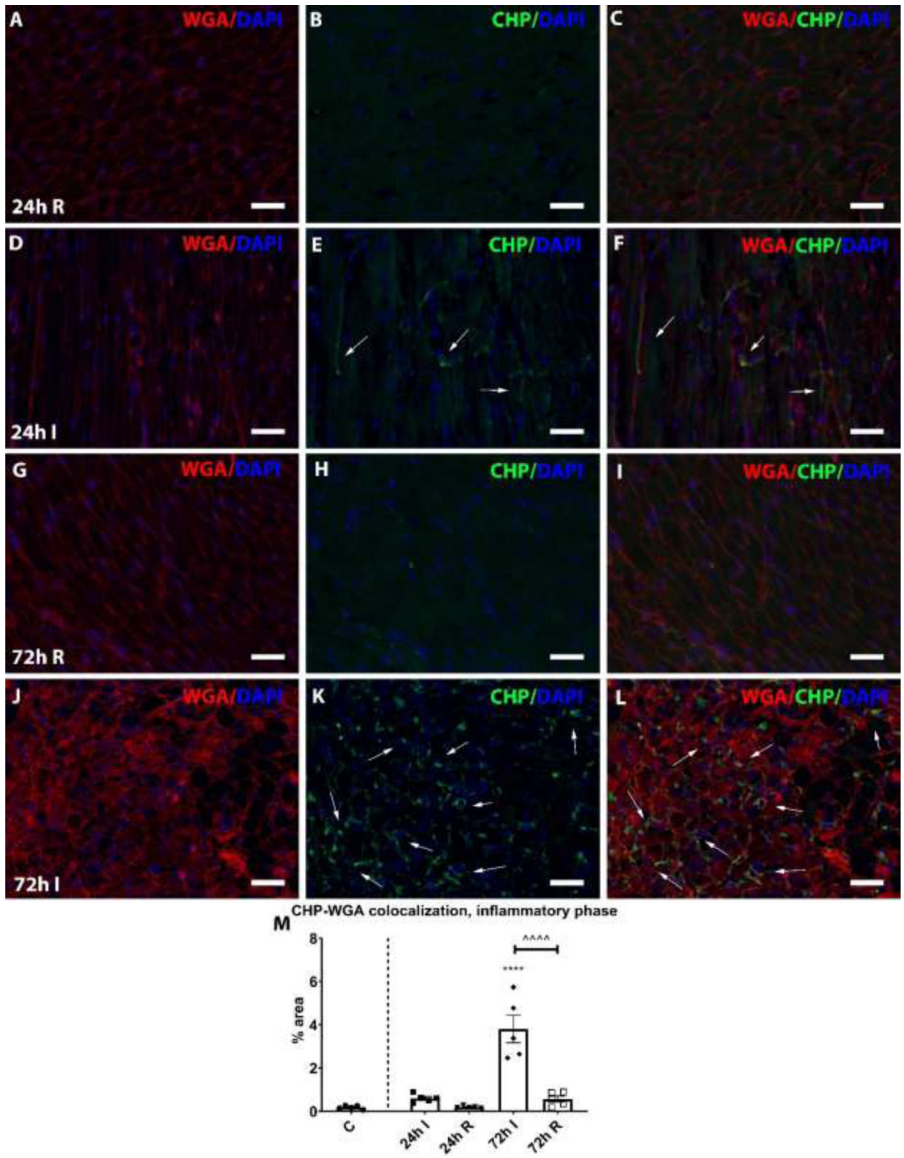

Figure 1: During the inflammatory phase of cardiac repair, collagen denaturation is restricted to the infarcted area and is localized in areas of inflammatory cell infiltration.

A–L: Representative images show the localization of denatured collagen (labeled using CHP staining) during the inflammatory phase of infarct healing (after 24–72h myocardial ischemia). WGA lectin histochemistry was used to label the cardiac interstitium. **A–C and G–I**, Remote non-infarcted areas showed no collagen denaturation after 24h (24h R) and 72h (72h R) of myocardial ischemia. In the infarct zone (I), low levels of denatured collagens were noted after 24h of myocardial infarction (arrows, 24h I, **D–F**). After 72h of coronary occlusion, there was significant increase in collagen denaturation in the infarct zone (arrows, 72h I, **J–L)**. Scalebar=50 μm. DAPI indicates 4′,6-diamidino-2-phenylindole. **M**, Quantitative analysis of the surface area of the colocalization of CHP-WGA shows a marked increase in collagen denaturation in the infarct zone (I) after 72h of myocardial ischemia (****P<0.0001 vs control, ^^^^P<0.0001, n=5/group).

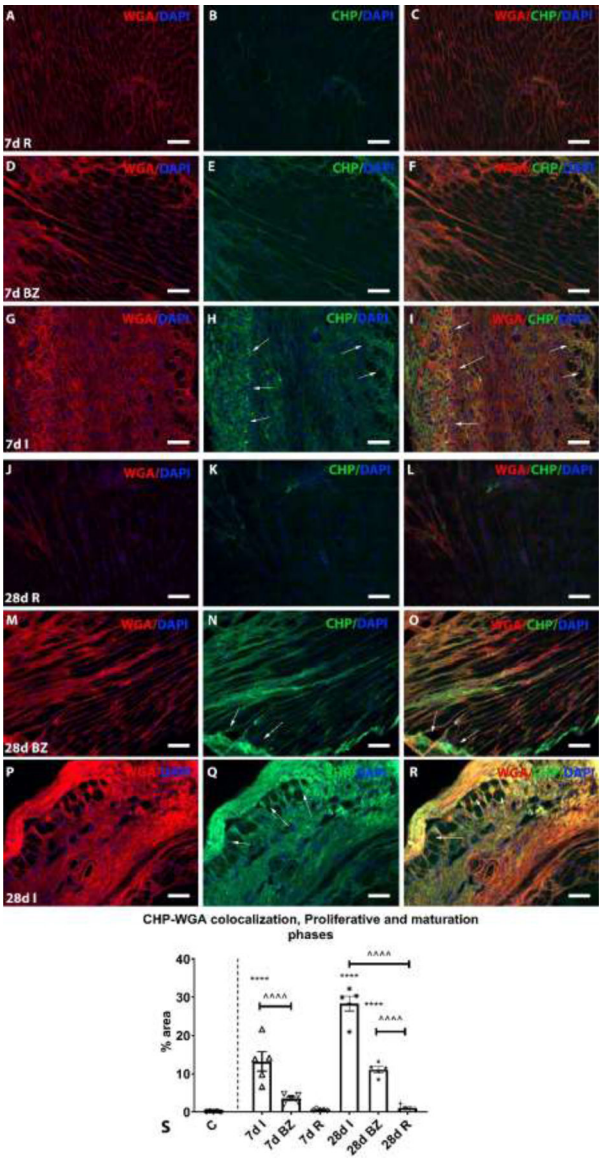

Figure 2: The time course and localization of denatured collagen during the proliferative and maturation phases of myocardial infarction.

A–I, During the proliferative phase of cardiac repair (7 days after coronary occlusion), denatured collagen was predominantly pericellular, and localized in the infarct border zone **(**7d BZ, **D–F)**, and in the highly cellular healing infarct **(**7d I, **G–I)**, but not in the remote myocardium (7d R, A–C). **J–R**, During the maturation phase (28 days after coronary occlusion), the scar has a low cellular content, but exhibits extensive collagen denaturation in the extracellular matrix of the infarct border zone **(**arrows, 28d BZ, **M–O)**, and the infarct **(**arrows, 28d I, **P–R)**, but not in the remote myocardium (28d R, J–L). **S**, Quantitative analysis of the surface area of CHP and WGA colocalization showed marked increase in collagen denaturation in the infarct after 7 days of coronary occlusion that increased further in mature scars after 28 days of coronary occlusion. *(****P<0.0001 vs control, ^^^^P<0.0001, n=5/group).* DAPI indicates 4′,6-diamidino-2-phenylindole. Scalebar=50 μm.

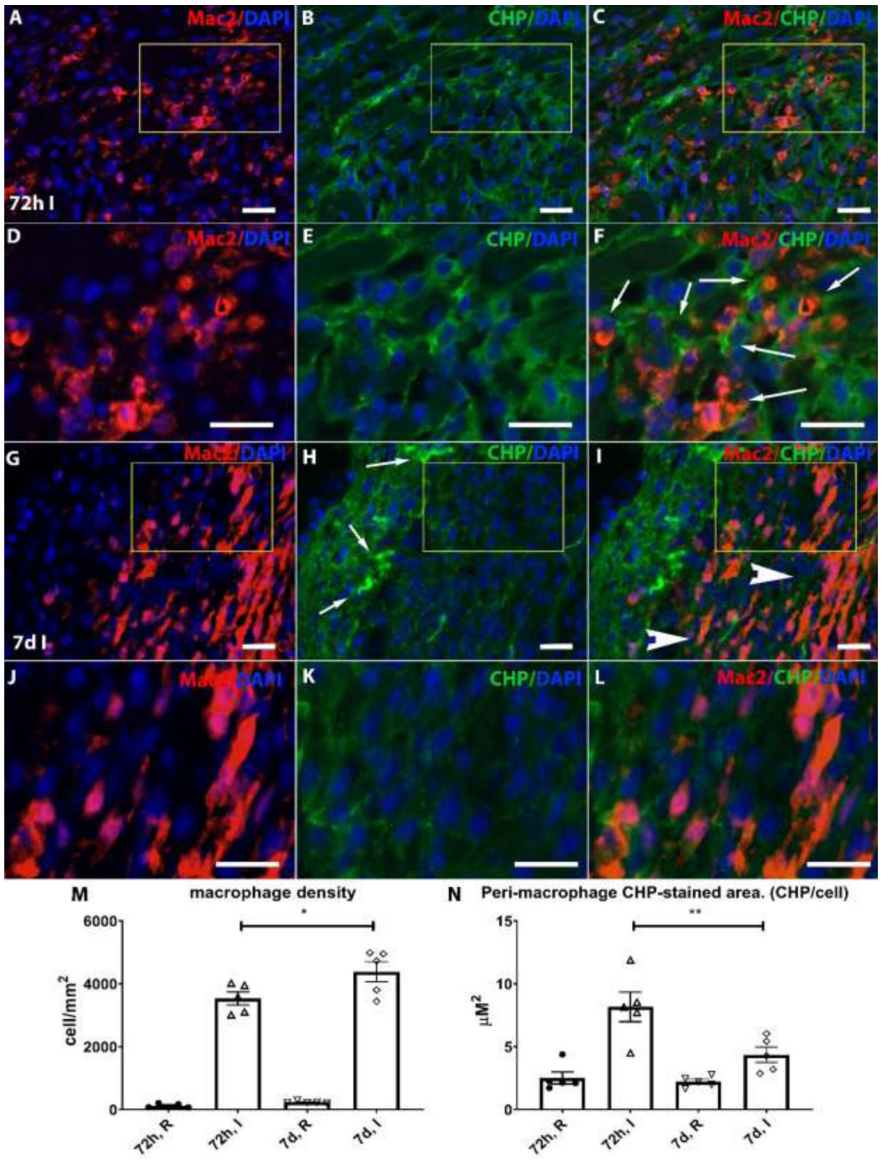

Figure 3: Macrophage-associated collagen denaturation peaks during the inflammatory phase of infarct healing.

Dual staining for the macrophage marker Mac2 and CHP showed that during the inflammatory phase of infarct healing (3 days after permanent occlusion), collagen denaturation was localized in close proximity to infiltrating macrophages (arrows, 72h I, **A–F)**. Collagen denaturation around macrophages decreased during the proliferative phase of infarct healing (7 days after permanent occlusion, 7d I, **G–L** arrowheads**)**. We quantified macrophage density **(M)** and peri-macrophage CHP stained areas **(N)** at 3 and 7 days after permanent occlusion. Macrophage density progressively increased in the infarct; however, peri-macrophage collagen denaturation peaked during the inflammatory phase after 3 days of coronary occlusion. *(*P=0.02, **P=0.008, n=5/group).* **D–F** and **J–L** are magnified images from the highlighted rectangles in **A–C** and **G–I** respectively. Scalebar=20 μm.

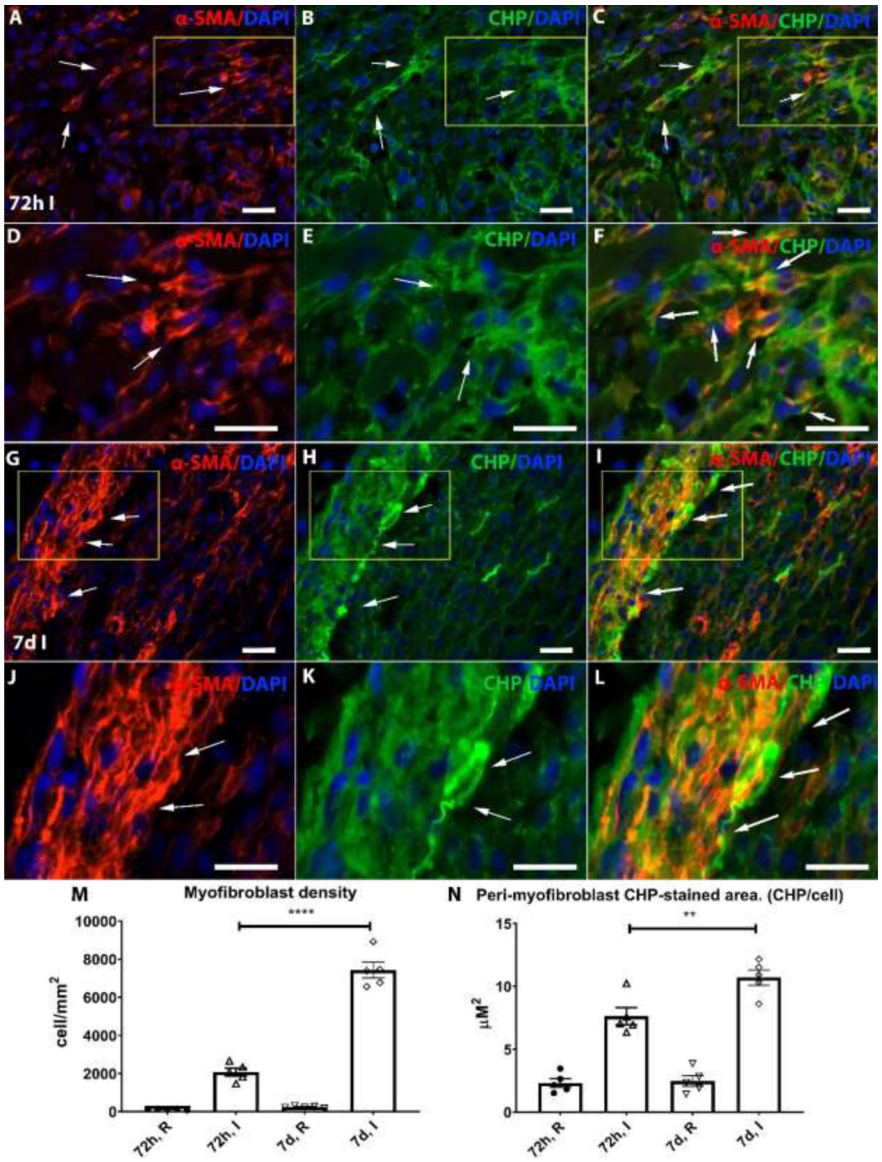

Figure 4: During the proliferative phase of infarct healing, denatured collagen is predominantly localized in association with α-SMA+ myofibroblasts.

α-SMA staining identified myofibroblasts as immunoreactive non-mural cells. Dual staining for the myofibroblast marker α-SMA and CHP showed collagen denaturation in close proximity to infarct myofibroblasts during the inflammatory phase **(**72h I, **A–F** arrows**)** that increased further during the proliferative phase of infarct healing **(**7d I, **G–L** arrows**)**. Quantification of myofibroblast density **(M)** in the infarct showed a progressive increase in myofibroblast density during the inflammatory and proliferative phase of healing. The amount of peri-myofibroblast denatured collagen progressively increased after 72h to 7 days of myocardial ischemia **(N)**. *(****P<0.0001, **P=0.004, n=5/group).* Scalebar=20 μm.

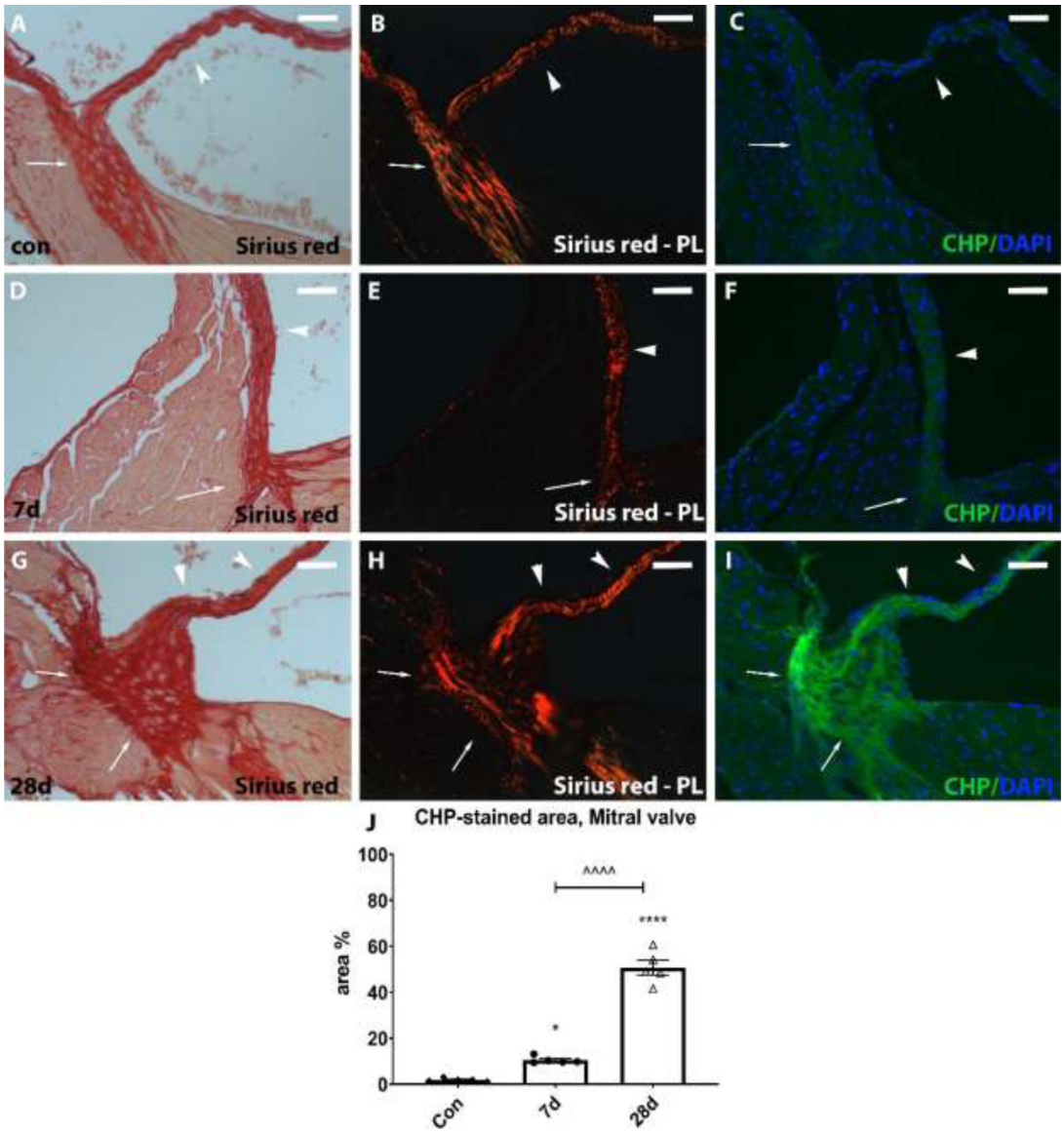

Figure 5: Dilative post-infarction cardiac remodeling is associated with collagen denaturation in the mitral valve annulus and in the leaflets, possibly reflecting mechanical stretch of the valve apparatus.

Myocardial sections were stained for Sirius red to label collagen fibers and were visualized under light microscopy (Sirius red - A, D, G) or with polarized light (Sirius red PL - B, E, H). Serial sections were stained for CHP (C, F, I) to label denatured collagen. Control hearts had negligible CHP labeling in the mitral valve annulus (arrows) and leaflets (arrowheads) **(A–C)**. Low level collagen denaturation was noted in the annulus (arrows) 7 days after coronary occlusion **(D–F)**. Collagen denaturation markedly increased after 28 days of coronary occlusion in the annulus (arrows) and in the leaflets (arrowhead), **(G–I)**. Collagen denaturation in the mitral valve annulus may reflect mechanical damage of the valvular extracellular matrix due to dilation of the infarcted ventricle. **J**, Quantification of the CHP-stained area showed that collagen denaturation in the mitral valve annulus peaks at

28 days following coronary occlusion. *(*P<0.05, ****P<0.0001 vs control, ^^^^P<0.0001, n=5/group).* Scalebar=50 μm.

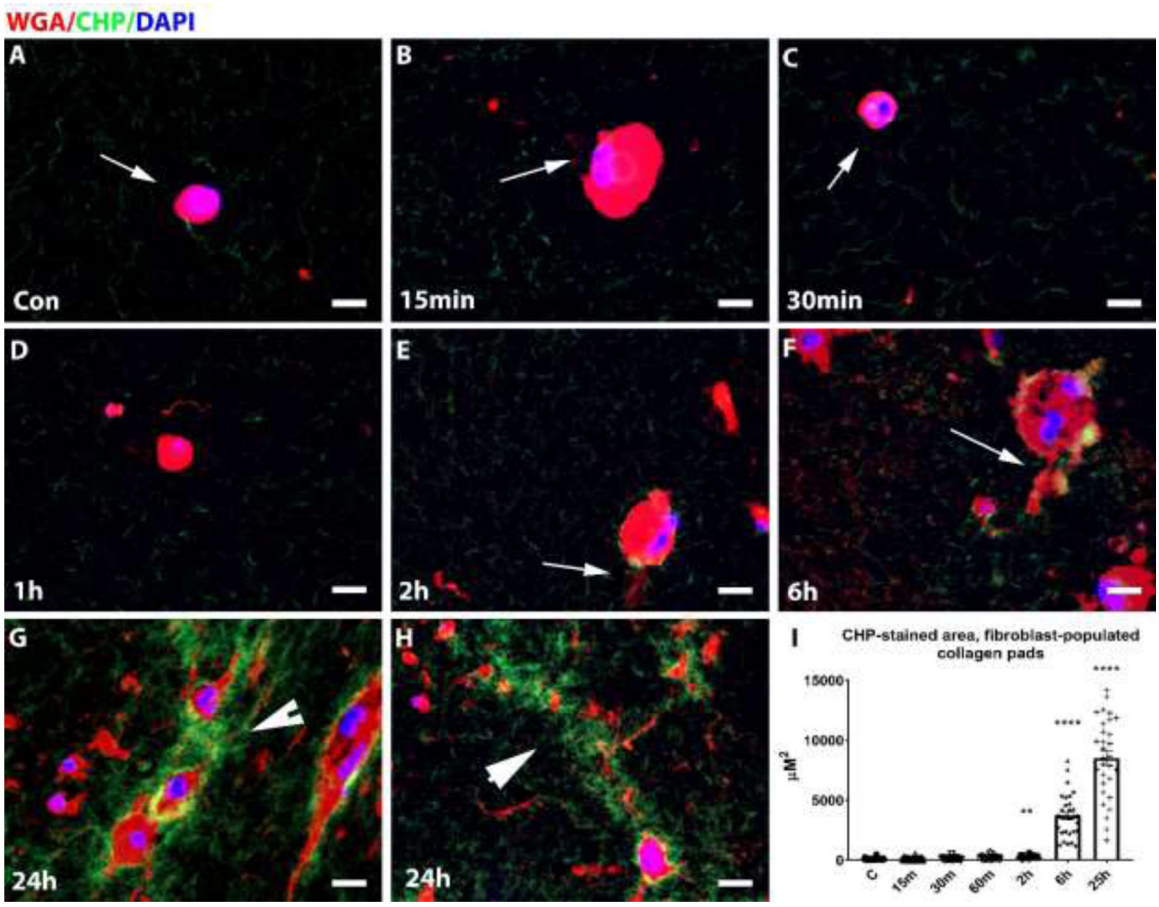

Figure 6: Fibroblasts populating collagen pads form tracks of denatured collagen after 24h of culture.

A–D, Cardiac fibroblasts cultured in free floating collagen lattices for 15'−60' exhibited a round morphology with no significant pericellular collagen denaturation. **E–F**, After 2h–6h in the pads, fibroblasts developed projections, and started to denature the surrounding collagen. **G–H**, At 24h, fibroblasts acquired a dendritic morphology, with a dramatic increase in pericellular collagen denaturation along the track of cell migration. **I**, Quantification of the pericellular CHP-labeled area showed a progressive increase in collagen denaturation, peaking after 24h of culture. *(**P<0.005, ****P<0.0001,* n=30 cells/group from 3 independent experiments*).* Wheat germ agglutinin (WGA) lectin histochemistry was used to label the fibroblasts (through binding to cytoplasmic and membrane glycoproteins) and DAPI was used as a nuclear marker. Scalebar=20 μm.

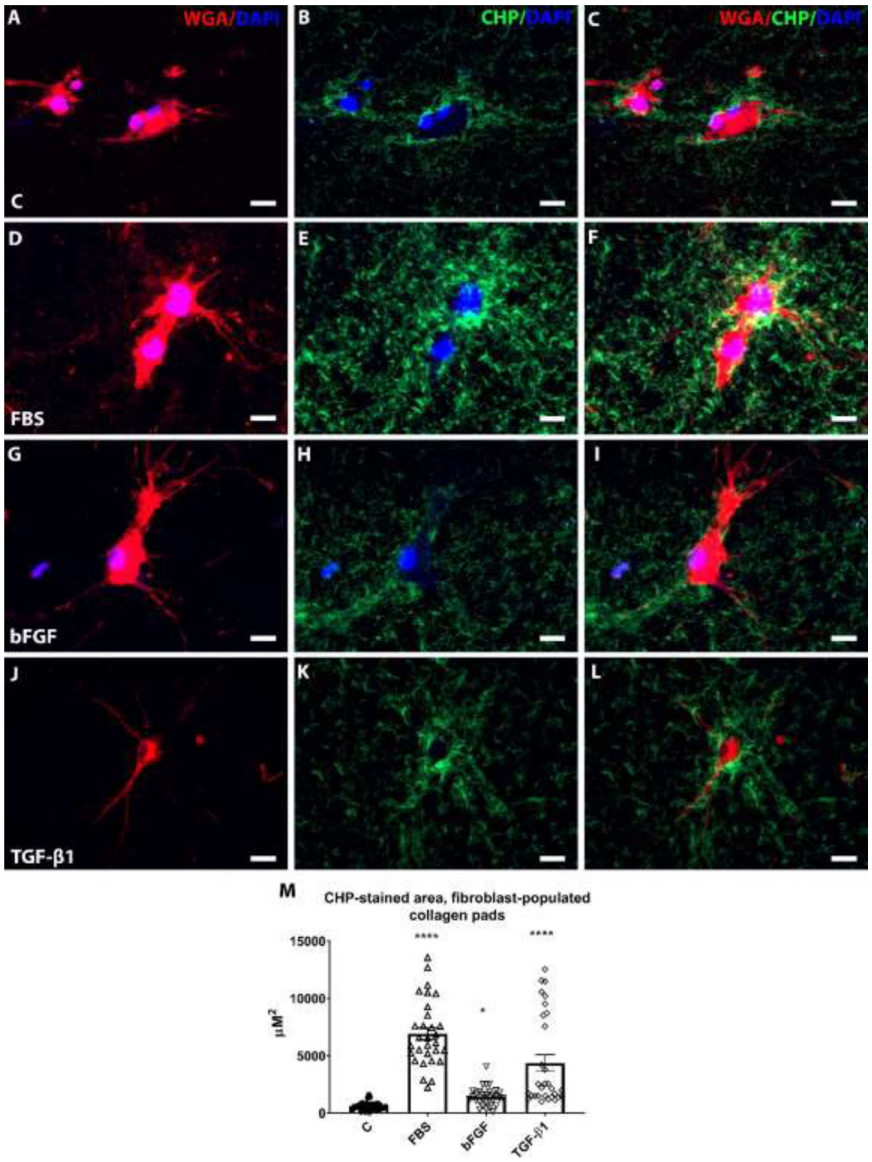

Figure 7: Effects of growth factors on collagen denaturation in fibroblast-populated collagen lattices.

Cardiac fibroblasts were cultured in free-floating collagen lattices for 24h in the presence or absence of growth factors. **A–C**, Low levels of collagen denaturation were noted in pads cultured in serum-free media. Stimulation with 10% fetal bovine serum (FBS) markedly increased the levels of pericellular denatured collagen in fibroblast-populated collagen pads (arrows) **(D–F)**, Stimulation with bFGF **(G–I)**, or TGF-β1 moderately, but significantly increased collagen denaturation (arrows) **(J–L)**. **M**, Quantification of the pericellular CHP-stained area showed that FBS, bFGF and TGF–β1 significantly increased pericellular collagen denaturation in fibroblast-populated lattices. *(*P<0.05, ****P<0.0001,* n=30 cells/group from 3 independent experiments*).* **Wheat germ agglutinin (**WGA) lectin histochemistry was used to label the fibroblasts (through binding to cytoplasmic and membrane glycoproteins) and **DAPI was used as a nuclear marker.** **Scalebar=20 μm.**

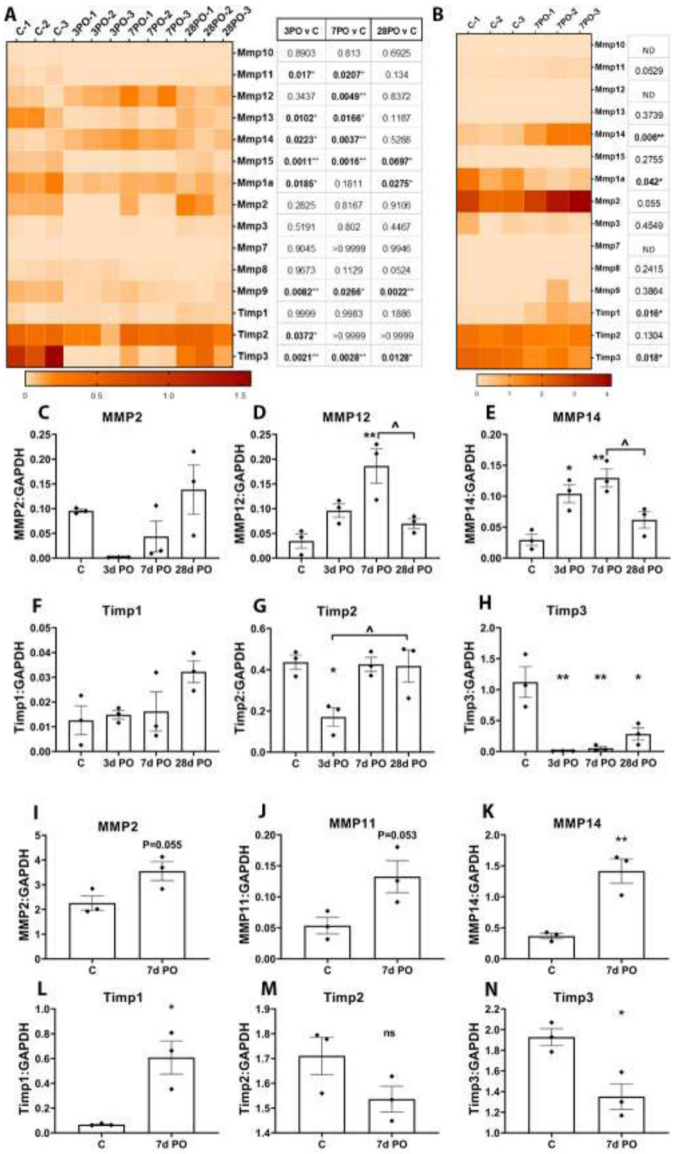

Figure 8: Expression of MMPs and TIMPs in cardiac macrophages and fibroblasts from control or infarcted hearts.

A, C–H, Heatmap and quantitative analysis show the relative expression of MMPs and TIMPs in CD11b+/Ly6G-macrophages isolated from control hearts (C) or after 3, 7, and 28 days of coronary occlusion (3d PO, 7d PO, and 28d PO respectively). **B, I–N,** Expression of MMPs and TIMPs in FACS sorted CD31−/CD45− cells (predominantly fibroblasts) from control hearts or 7 days following myocardial infarction. MMP14 (MT1-MMP) expression is markedly upregulated in infarct macrophages (3–7days after infarction) **(A, E)**, and in infarct fibroblasts (7 days post-infarction) **(B, K),** compared to corresponding control cells. P values are tabulated next to the corresponding heatmaps and the p-values of the genes with statistically significant differential expression are highlighted in bold, *(ND= gene expression was not detected in the qPCR arrays, *P<0.05, **P<0.01 vs. control, ^P<0.05,* n=3/group*).*

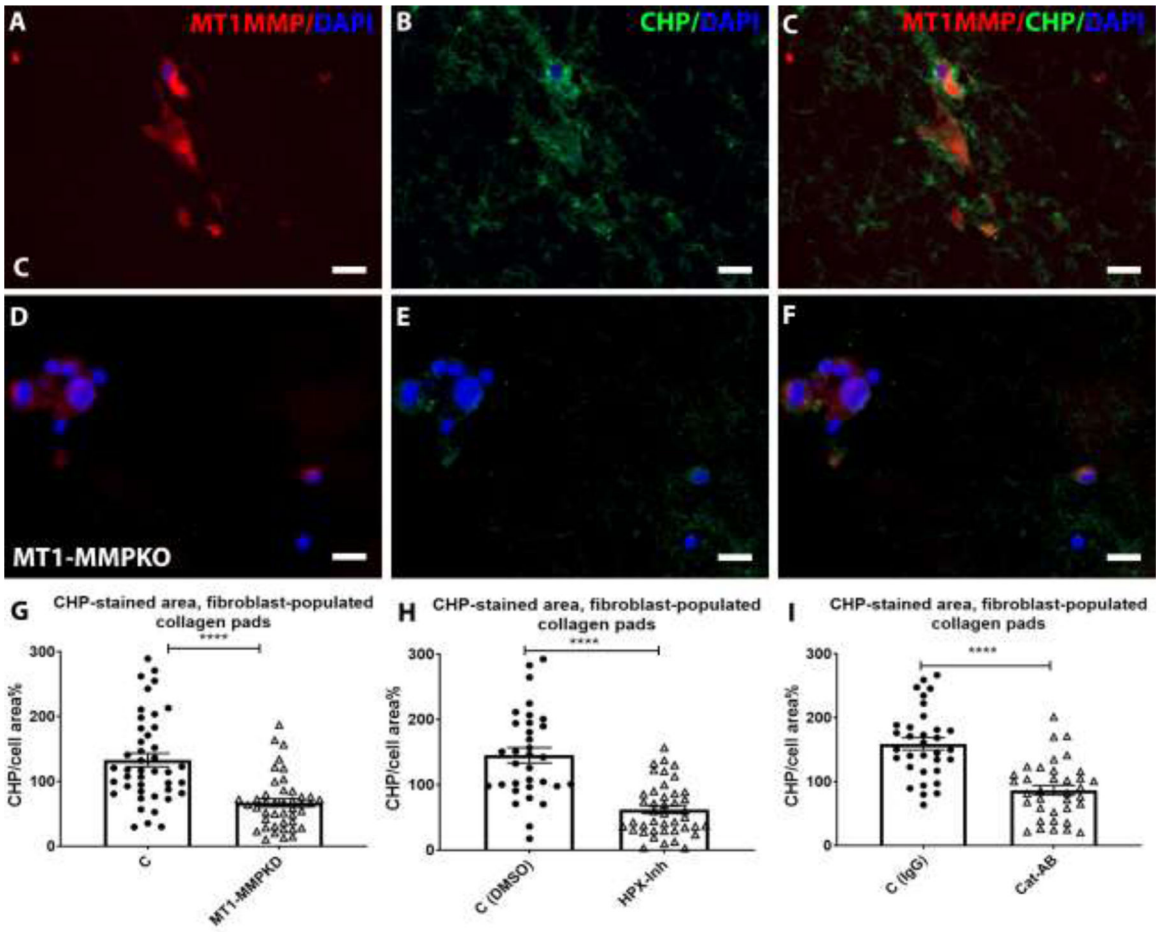

Figure 9: Pericellular collagen denaturation in fibroblast-populated collagen pads is dependent on MT1-MMP, and mediated through its hemopexin and catalytic domains.

A–C: Dual staining for CHP and MT1-MMP demonstrated that pericellular collagen denaturation in fibroblast-populated collagen pads was associated with MT1-MMP expression. **D–G**, MT1-MMP knockdown (MT1-MMP KD) using siRNA in cardiac fibroblasts that were subsequently cultured in collagen pads showed that pericellular collagen denaturation is dependent on MT1-MMP. The mechanism of MT1-MMP-mediated collagen denaturation was dissected through experiments inhibiting the MT1-MMP hemopexin domain (using a functional inhibitor), and through catalytic domain blockade with a neutralizing antibody. G–I, Quantitative analysis showed that knockdown of MT1-MMP **(MT1-MMPKD, G)**, inhibition of MT1-MMP hemopexin domain **(HPX-Inh, H)**, or antibody-mediated blockade of MT1-MMP catalytic domain **(Cat-AB, I)** all markedly reduced pericellular denatured collagen levels in fibroblasts cultured in collagen pads. *(****P<0.0001,* n=33–43 cells/group from 3 independent experiments*).* DAPI was used as a nuclear marker. Scalebar=20 μm.

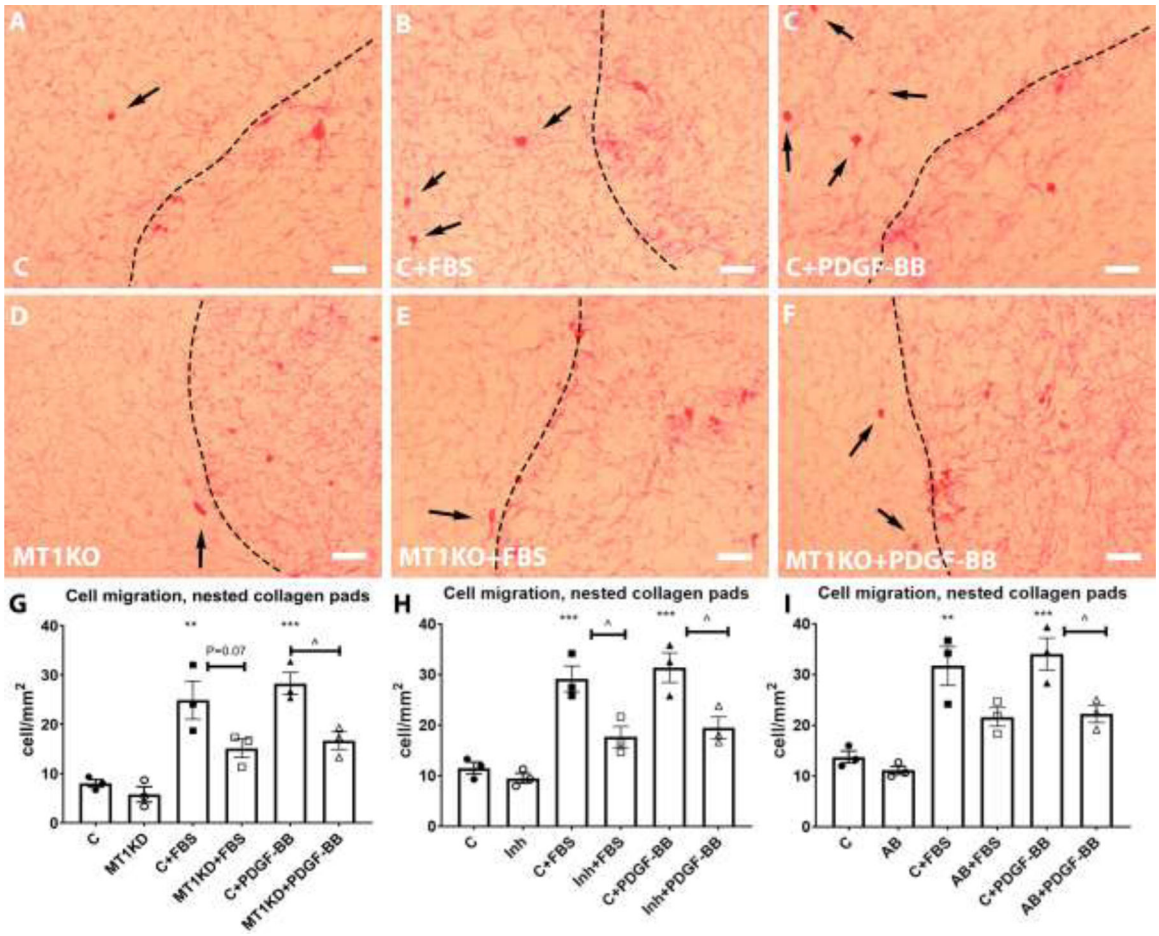

Figure 10: MT1-MMP inhibition attenuates fibroblast migration in a nested pad model.

A–F: A fibroblast migration assay was developed using a model of nested collagen pads: a fibroblast-populated inner lattice was nested into another acellular outer lattice, allowing cells to migrate from the inner to the outer matrix in response to growth factor stimulation. The effects of MT1-MMP on cell migration were examined through siRNA knockdown (MT1KD). The mechanism of MT1-MMP effects on cell migration was explored through functional inhibition of the MT1-MMP hemopexin domain (Inh), or antibody-mediated blockade of the MT1-MMP catalytic domain (AB). Quantification of numbers of migrating cells in the outer matrix **(G–I)** showed that in the absence of growth factor stimulation there was no difference in cell migration between control and MT1-MMP KD cells **(A,D)**. Knockdown of MT1-MMP **(D)**, inhibition of MT1-MMP hemopexin domain **(H)**, or antibody mediated blockage of MT1-MMP catalytic domain **(I)** all attenuated fibroblast migration in response to stimulation with fetal bovine serum **(**FBS, **B,E)**, or platelet-derived growth factor-BB (PDGF-BB, **C,F)**. Sirius red staining with eosin counterstain was used to stain the collagen pads and to identify the fibroblasts. *(**P<0.001, ***P<0.0001, ^P<0.05 vs control ^P<0.05 vs the corresponding controls, P=0.07 in MT1KD+FBS vs C+FBS, n=3/group).* Scalebar=50 μm.

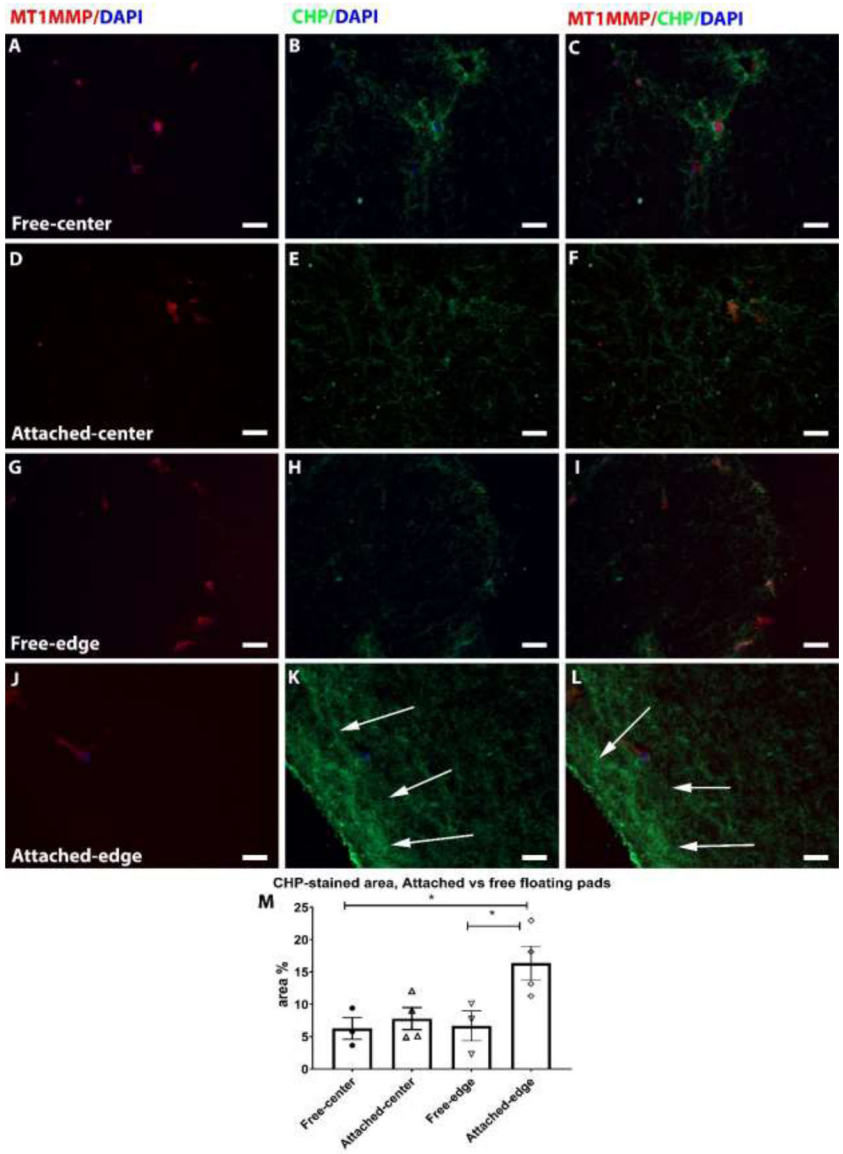

Figure 11: In attached fibroblast-populated collagen lattices, mechanical stress induces peripheral collagen denaturation in the absence of MT1-MMP.

In order to examine whether mechanical tension can cause collagen denaturation, we compared CHP labeling between free-floating pads (in which tension is low) and attached pads (which are associated with a high-tension environment). Collagen denaturation levels were comparable in the center of low-tension free-floating pads (Free-center) and high-tension attached pads (Attached-center) **(A–F, M)**. However, the edges of the high-tension attached pads (Attached-edge) exhibited markedly increased collagen denaturation (arrows) compared to the edges of the low-tension free-floating pads (Free-edge) **(G–L, M)**. *(*P<05, n=3–4/group).* Collagen denaturation in attached pads was not associated with an increase in MT1-MMP immunoreactivity. Immunostaining with an anti-MT1-MMP antibody was used to localize MT1-MMP, CHP was used to label denatured collagen and DAPI was used as a nuclear stain. Scalebar=50 μm.

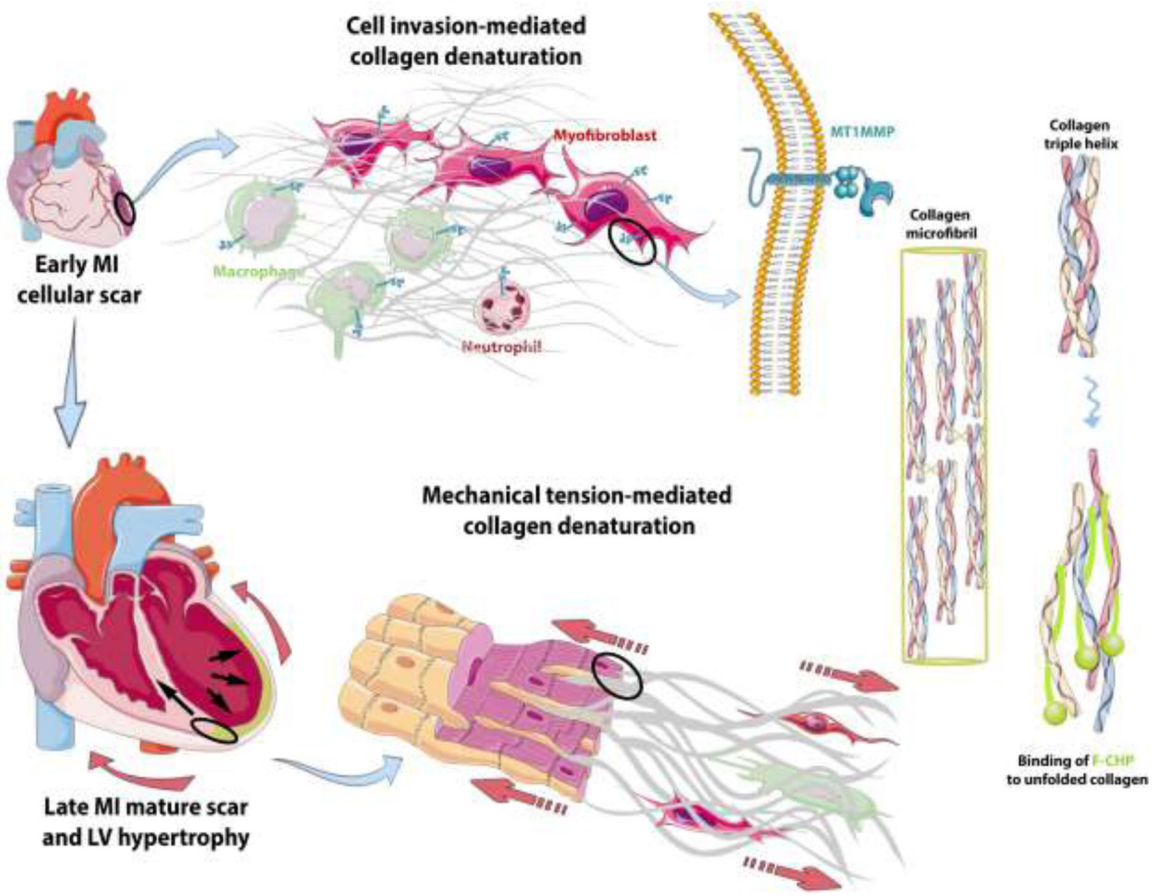

Figure 12: Mechanisms of collagen denaturation in healing myocardial infarction. Our findings suggest two distinct mechanisms of collagen denaturation in healing infarcts.

During the inflammatory and proliferative phase of myocardial infarction, collagen denaturation is pericellular, reflecting migration of inflammatory cells and reparative myofibroblasts. Cell migration and collagen denaturation are dependent on MT1-MMP expression. Pericellular collagen denaturation may be important for repair of the infarcted heart by facilitating infiltration with phagocytic macrophages and matrix-producing fibroblasts. Surprisingly, as the scar matures, collagen denaturation increases further and is localized in hypocellular areas of the matrix subjected to mechanical tension (such as the subepicardial areas, the border zone and the mitral valve apparatus). Chronic mechanical damage of the extracellular matrix and unfolding of collagen chains may increase susceptibility to proteolysis, contributing to the pathogenesis of adverse remodeling.